Author/s:
Preston, S;Korhonen, PK;Mouchiroud, L;Cornaglia, M;McGee, SL;Young, ND;Davis, RA;Crawford, S;Nowell, C;Ansell, BRE;Fisher, GM;Andrews, KT;Chang, BCH;Gijs, MAM;Sternberg, PW;Auwerx, J;Baell, J;Hofmann, A;Jabbar, A;Gasser, RB

Title:
Deguelin exerts potent nematocidal activity via the mitochondrial respiratory chain

Date:
2017-10-01

Citation:
Preston, S., Korhonen, P. K., Mouchiroud, L., Cornaglia, M., McGee, S. L., Young, N. D., Davis, R. A., Crawford, S., Nowell, C., Ansell, B. R. E., Fisher, G. M., Andrews, K. T., Chang, B. C. H., Gijs, M. A. M., Sternberg, P. W., Auwerx, J., Baell, J., Hofmann, A., Jabbar, A. & Gasser, R. B. (2017). Deguelin exerts potent nematocidal activity via the mitochondrial respiratory chain. FASEB Journal, 31 (10), pp.4515-4532. https://doi.org/10.1096/fj.201700288R.

The FASEB Journal article fj.201700288R. Published online July 7, 2017.

THE FASEB JOURNAL • RESEARCH • www.fasebj.org

Deguelin exerts potent nematocidal activity *via* the mitochondrial respiratory chain

Sarah Preston,[*,†] Pasi K. Korhonen,[*] Laurent Mouchiroud,[‡] Matteo Cornaglia,[§] Sean L. McGee,[¶] Neil D. Young,[*] Rohan A. Davis,[‖] Simon Crawford,[#] Cameron Nowell,[**] Brendan R. E. Ansell,[*] Gillian M. Fisher,[‖] Katherine T. Andrews,[‖] Bill C. H. Chang,[*,††] Martin A. M. Gijs,[§] Paul W. Sternberg,[‡‡] Johan Auwerx,[‡] Jonathan Baell,[§§] Andreas Hofmann,[*,‖] Abdul Jabbar,[*] and Robin B. Gasser[*,1]

[*]Faculty of Veterinary and Agricultural Sciences, University of Melbourne, Parkville, Victoria, Australia; [†]Faculty of Science and Technology, Federation University, Ballarat, Victoria, Australia; [‡]Laboratory of Integrative and Systems Physiology and [§]Laboratory of Microsystems, École Polytechnique Fédérale de Lausanne, Lausanne, Switzerland; [¶]Metabolic Research Unit, Metabolic Reprogramming Laboratory, School of Medicine, Faculty of Health, Deakin University, Waurn Ponds, Victoria, Australia; [‖]Griffith Institute for Drug Discovery, Griffith University, Nathan, Queensland, Australia; [#]School of Biosciences, University of Melbourne, Parkville, Victoria, Australia; [**]Drug Discovery Biology and [§§]Medicinal Chemistry, Monash University Institute of Pharmaceutical Sciences, Monash University, Parkville, Victoria, Australia; [††]Yourgene Bioscience, Taipei, Taiwan; and [‡‡]Division of Biology and Biological Engineering, California Institute of Technology, Pasadena, California, USA

ABSTRACT: As a result of limited classes of anthelmintics and an over-reliance on chemical control, there is a great need to discover new compounds to combat drug resistance in parasitic nematodes. Here, we show that deguelin, a plant-derived rotenoid, selectively and potently inhibits the motility and development of nematodes, which supports its potential as a lead candidate for drug development. Furthermore, we demonstrate that deguelin treatment significantly increases gene transcription that is associated with energy metabolism, particularly oxidative phosphorylation and mito-ribosomal protein production before inhibiting motility. Mitochondrial tracking confirmed enhanced oxidative phosphorylation. In accordance, real-time measurements of oxidative phosphorylation in response to deguelin treatment demonstrated an immediate decrease in oxygen consumption in both parasitic (*Haemonchus contortus*) and free-living (*Caenorhabditis elegans*) nematodes. Consequently, we hypothesize that deguelin is exerting its toxic effect on nematodes as a modulator of oxidative phosphorylation. This study highlights the dynamic biologic response of multicellular organisms to deguelin perturbation.—Preston, S., Korhonen, P. K., Mouchiroud, L., Cornaglia, M., McGee, S. L., Young, N. D., Davis, R. A., Crawford, S., Nowell, C., Ansell, B. R. E., Fisher, G. M., Andrews, K. T., Chang, B. C. H., Gijs, M. A. M., Sternberg, P. W., Auwerx, J., Baell, J., Hofmann, A., Jabbar, A., Gasser, R. B. Deguelin exerts potent nematocidal activity *via* the mitochondrial respiratory chain. FASEB J. 31, 000–000 (2017). www.fasebj.org

KEY WORDS: natural product · anthelmintic activity · transcriptomics · oxidative phosphorylation · nematode

The widespread resistance of parasitic worms of livestock animals to commonly used anthelmintics necessitates continued efforts to discover new effective chemicals for subsequent commercial development, particularly those with new modes of action to limit cross-resistance (1). Natural products have enormous chemical and structural diversity that is unmatched by synthetic sets of small molecules (2). Such products are considered evolutionarily optimized drug-like molecules and continue to be an excellent source of new drugs (3). Although there have been considerable advances in antiparasite treatments—for example, through the early discoveries of avermectins and artemisinin by William Campbell, Satoshi Omura, and Youyou Tu, who were jointly awarded the Nobel Prize in 2015—there has been relatively little progress since the 1960s. Unfortunately, many pharmaceutical companies have reduced or eliminated their natural product programs, in part because of the advent of high-throughput screening and combinatorial synthesis technologies, which allows large synthetic libraries of small molecules to be constructed and screened (2). For many years, relatively disappointing results were obtained using the latter approach; however, today, this approach is highly successful (4). Recognition that biologically relevant chemical diversity is crucial—combined with progress in genomics, bioinformatics—the biosynthesis of natural products and the availability of advanced analytical techniques are

ABBREVIATIONS: KEGG, Kyoto Encyclopedia of Genes and Genomes; LB, Luria Bertani; L3, third-stage larva; L4, fourth-stage larva; NFF, neonatal foreskin fibroblast; NGM, nematode growth medium; SEM, scanning electron microscopy; SI, selectivity index; TMRE, tetramethylrhodamine ethyl ester; UPR^{mt}, mitochondrial unfolded protein response

[1] Correspondence: Faculty of Veterinary and Agricultural Sciences, University of Melbourne, Parkville, VIC 3010, Australia. E-mail: robinbg@unimelb.edu.au

doi: 10.1096/fj.201700288R
This article includes supplemental data. Please visit *http://www.fasebj.org* to obtain this information.

driving a renewed interest in pursuing natural products for drug discovery. This is particularly the case for anthelmintics and other antiparasitic and antibiotic agents, which are naturally aligned with Nature's need to develop a chemical warfare arsenal (5).

In a recent pilot study, we screened a small set of compounds that were derived from natural products against parasitic larval stages of the barber's pole worm, *Haemonchus contortus*, of ruminants, and identified deguelin as having submicromolar activity against this nematode *in vitro* (unpublished results). *H. contortus* is a highly pathogenic, blood-feeding parasitic worm that has a major economical impact on ruminant production worldwide. It feeds on blood in the stomach and causes gastritis, anemia, and associated complications, which leads to serious production losses and death in severely affected animals. The parasite has a direct life cycle and is transmitted *via* a fecal-oral route in which animals are infected by third-stage larvae (L3s) from contaminated pasture: infective L3s ingested by the host exsheath (shed outer cuticle; xL3) and develop through to fourth-stage larvae (L4s) to dioecious adults (within 3 wk) in the abomasum. Adult worms within the stomach then mate and the female will produce eggs, which are excreted by the host in feces; individual first-stage larvae (L1s) develop inside eggs, then hatch (usually within 1 d) and develop through to the second-stage larvae and L3s in approximately 1 wk.

Deguelin and other rotenoids—for example, rotenone and tephrosin—of the flavonoid group are derived from plants of the family Leguminosae (*e.g.*, *Lonchocarpus*, *Derris*, *Cassia*, and *Tephrosia*) (6–10). For example, resins that contain rotenoids extracted from the roots of *Lonchocarpus utiliz* (Cubé), *Lonchocarpus urucu* (Barbasco), *Derris elliptica* (Tuba plant), or *Derris involuta* (Jewel vine) have been used in many countries as natural insecticides, acaricides, and/or piscicides (11, 12). Deguelin also has therapeutic effects against a range of cancers—for example, in lung, stomach, and prostate—being able to inhibit tumor progression (13–19) with potent apoptotic and antiangiogenic activities *in vitro* (20). Deguelin is also used to improve the success of organ transplantation by reducing associated inflammation (21).

Although there were some early concerns about the safety of using deguelin in mammals as a result of the lethal effect of the analog rotenone on fishes and arthropods (13, 14), and because of Parkinson's disease–like symptoms in mice after chronic administration of deguelin (6 mg/kg/d) (22), no appreciable levels of toxicity or adverse effects of deguelin at therapeutic doses (2–5 mg/kg) have been recorded in rodents (mice and rats) (15, 17, 23, 24). Deguelin has been reported to exert its effects on rapidly replicating cells. For instance, it has been reported to inhibit tumor cell growth by targeting the PI3K/AkT and ERK signaling pathways (24–26), the IGF receptor pathway by inhibiting the binding of ATP to heatshock protein 90 clients proteins (27–29), and the glycogen synthase kinase-3β/β-catenin pathway by inhibiting the growth and survival of prostate cancer cells (30). Deguelin can also reduce tumor growth and metastasis in mice by inducing apoptosis and by inhibiting epithelial-to-mesenchymal transition by targeting the TGF-β1 and NF-κB signaling pathway (17, 31).

At the biochemical level, deguelin has been demonstrated to inhibit phorbol ester–induced ornithine decarboxylase activity (6, 13) as well as oxygen consumption by down-regulating NADH:ubiquinone or complex I of the mitochondrial electron transport chain in bovine heart cells, a human breast cancer cell line (MCF-7), and a human liver carcinoma cell line (HepG2) (6, 32, 33). In contrast, nothing is known about how deguelin affects parasitic nematodes. The relative *in vivo* safety of deguelin in mammals and, specifically, in rodent models of cancer at therapeutic doses (15, 17, 23, 24), the possibility of synthesizing analogs to alleviate the toxic properties that have been observed using excessive doses (27, 34, 35), and the potency of deguelin against *H. contortus* that was observed in our preliminary work (unpublished results) set the scene for the present investigation. Here, we *i*) describe the screening of a unique and well-defined library of natural products, including deguelin; *ii*) characterize the anthelmintic effect of deguelin on parasitic larvae of *H. contortus*; and *iii*) explore the molecular differences between treated and untreated larvae by using transcriptomic and biochemical approaches to understand how this chemical affects biologic pathways in this parasitic nematode.

MATERIALS AND METHODS

Procurement of *H. contortus*

L3s and L4s of *H. contortus* (Haecon-5 strain) were cultured from the feces of monospecifically infected sheep as previously described (36, 37). Approval to infect sheep was given by the University of Melbourne (Permit 1413429).

Screening of the compounds on *H. contortus* larvae *in vitro*

A natural product library that contained 260 compounds was purchased from Compounds Australia (www.griffith.edu.au/science-aviation/compounds-australia). This unique open-access library was established in 2010 by R.A.D. and, at the time of the present study, consisted of 260 distinct small molecules. The majority of the library compounds (~55%) have been purified from Australian natural sources, such as fungi (38), marine invertebrates (39), and plants (40). Approximately 30% of this library contained semisynthetic natural product analogs (41), whereas ~15% were known commercial drugs or synthetic compounds that were inspired by natural products. All compounds (purity > 95%) were supplied at a concentration of 5 mM in DMSO (Ajax Finechem, Taren Point, NSW, Australia) and diluted to a final concentration of 20 μM of compound and 0.5% of DMSO in Luria Bertani (LB) medium that was supplemented with 1% antibiotics-antimycotic mix (1000 U/ml penicillin, 1000 μg/ml streptomycin, and 2.5 μg/ml amphotericin B; Thermo Fisher Scientific, Waltham, MA, USA). This supplemented medium was designated LB* (36). Test compounds were transferred by using a multichannel pipette (Finnpipette; Thermo Fisher Scientific Life Sciences) into 96-well flat-bottomed microplates (Corning 3650; Corning, Corning, NY, USA) in a volume of 50 μl. Test and positive control compounds monepantel (Zolvix; Novartis Animal Health, Basel, Switzerland) and moxidectin (Cydectin; Virbac, Carros, France) were tested in triplicate on exsheathed L3s by using previously published methods (36, 37). Negative controls, LB*, and LB* + 0.5% DMSO were tested in replicates of 6. A volume of 50 μl that contained ~300 exsheathed

L3s was then transferred to each well by using a multichannel pipette (Finnpipette). Plates were incubated for 72 h at 38°C and 10% CO_2, then monitored for movement by videographic image analysis, from which a motility index was derived (36, 37). A compound was recorded as having anti–exsheathed L3 activity if it reduced motility by ≥70% at 72 h. Compounds with anti–exsheathed L3 activity were screened twice at 20 μM to verify their inhibitory properties on motility.

Testing of deguelin on *H. contortus* larvae

To determine the 50% inhibitory concentration [IC_{50} values of (−)-deguelin, purity ≥ 95%; Enzo Life Sciences, Basel, Switzerland] on larval motility and L4 development, this chemical was serially diluted 2-fold in LB*, starting at a concentration of 100 μM, as described previously (36, 37). The motility of exsheathed L3s was recorded 24, 48, and 72 h after exposure to the chemical (36, 37). Seven days after incubation with deguelin, the development of exsheathed L3s to L4s was assessed by microscopic assessment of the presence or absence of a buccal capsule and directly compared with negative control (LB* + 1% DMSO). To establish IC_{50} values, compound concentrations were log_{10}-transformed, multiplied by 10, and a variable slope 4-parameter equation was used, which constrained the top to 100% (Prism v.7.01; GraphPad Software, La Jolla, CA, USA). A 2-way ANOVA and the Dunnett's multiple comparison test were used to compare the effects of compounds on motility and larval development at different concentrations and time points. All experiments were performed in triplicate on 3 separate days.

Testing of cell toxicity and selectivity *in vitro*

Cell toxicity was assessed as described previously (42). In brief, neonatal foreskin fibroblast (NFF) cells were cultured in RPMI 1640 medium (Thermo Fisher Scientific) that was supplemented with 10% fetal calf serum (CSL Biosciences, Parkville, VIC, Australia) and 1% streptomycin (Thermo Fisher Scientific). The inhibition of growth (%) was compared with matched DMSO controls. IC_{50} values were calculated by using linear interpolation of inhibition curves. Mean IC_{50} value (± SD) was recorded in 3 independent experiments, each carried out in triplicate wells. The selectivity index (SI) was calculated as IC_{50} for NFF divided by IC_{50} for *H. contortus*.

Scanning electron microscopy

Scanning electron microscopy (SEM) was used to assess whether deguelin causes structural damage to the larval stages of *H. contortus*, as previously described (43). In brief, deguelin and positive control compounds—monepantel and moxidectin—were each diluted to a final concentration of 100 μM in LB* and incubated with exsheathed L3s or L4s in wells of a 96-well plate at a density of 6000 larvae/ml for 24 h at 38°C and 10% CO_2. Subsequently, worms were washed three times in physiologic saline, resuspended in PBS, processed, and fixed for SEM.

Deguelin treatment of *H. contortus* exsheathed L3s and RNA isolation

On 4 different days (biologic replicates), 3 technical replicates of untreated exsheathed L3s and deguelin-treated exsheathed L3s were prepared. Untreated exsheathed L3s were produced by adding 30,000 exsheathed L3s in 1 ml of LB* + 0.25% DMSO to each of 3 wells of a 24-well plate (Corning), and deguelin-treated exsheathed L3s were produced by adding the same number of exsheathed L3s in 1 ml of LB* + 0.25% DMSO + 12.5 μM of deguelin to the same number of wells. All exsheathed L3s were incubated at 38°C with 10% CO_2 for 48 h. For each of the 4 biologic replicates of both untreated exsheathed L3s and deguelin-treated exsheathed L3s, the 3 technical replicates were pooled (total volume), centrifuged, supernatants were removed, 2 ml of Trizol reagent (Thermo Fisher Scientific) were added, homogenized for 2 min by using a rotary tissue homogenizer (IKA, Plaisir, France), then frozen at −80°C until further processing. Subsequently, total RNA was isolated from the 8 samples according to the manufacturer's instructions (Trizol reagent). All RNA samples were treated with DNase (Turbo-DNAfree; Thermo Fisher Scientific) to remove any possible genomic DNA from *H. contortus*. RNA quality in each sample was evaluated by using a fluorometer (Qubit 3.0; Thermo Fisher Scientific) and by electrophoretic analysis (70 V for 45 min) in 1% agarose gel, employing a 1-kb ladder (Promega, Madison, WI, USA) as a size marker.

RNA-sequencing, transcriptome assembly, and analyses

The 4 biologic replicates representing deguelin-untreated exsheathed L3s and the 4 representing deguelin-treated exsheathed L3s were all subjected to RNA sequencing as described previously (44). In brief, libraries were built by using the TruSeq-stranded mRNA library kit (Illumina, San Diego, CA, USA) and paired-end sequenced using the Illumina HiSeq 2500 platform at Yourgene Bioscience. The quality of the reads that were obtained by sequencing from each of the 8 mRNA libraries was assessed using the program FastQC (*http://www.bioinformatics.babraham.ac.uk/projects/fastqc*). Poor-quality reads and adaptors were removed by using Trimmomatic (v.0.36) (45) that employed the following parameters: illumina clip = TruSeq3-PE.fa:2:30:10, leading = 3, trailing = 3, sliding window = 4:15, minlen = 36. The transcriptome was assembled separately by using the programs Velvet (v1.2.07) (46) and OASES (v.0.2.08) (47) using the following parameters: kmer = 25 and cov_cutoff = 12. Redundancy in the resultant assembly was reduced by using the program CD-HIT-EST (v.4.6) (48), employing the parameter $c = 0.9$. The basic local alignment search tool (BLASTp; E-value, 10^{-05}) (49) was used to scan remaining transcripts that encode homologous genes of *H. contortus*, and matching transcripts were preserved. High-quality reads from each library were mapped to the *H. contortus* transcriptome (50) by using the software package RSEM (v1.2.31) (51) employing the commands "rsem-prepare reference" and "rsem-calculate-expression" using the following parameters: bowtie2 p 24, paired-end, and bowtie2-mismatch-rate 0.2. The quality of the reads that mapped to the nonredundant transcriptome was assessed by using Picard Tools (http://picard.sourceforge.net), and the statistical package edgeR (v.3.14.0) (52) was used to identify differentially transcribed genes using a corrected a value of $P \leq 0.01$. To examine the effect of treatment on transcription, a hierarchical cluster was performed by using Euclidean distances employing the heatmap.2 function in the R package gplots (v.3.0.1; The R Foundation, Vienna, Austria). All transcripts that mapped to the nonredundant transcriptome were annotated by BLASTp (v.2.2.30+; E-value: 10^{-05}) against public gene and protein databases, including the National Center for Biotechnology Information (NCBI) nonredundant database (April 28, 2016) (53), Kyoto Encyclopedia of Genes and Genomes (KEGG; March 11, 2016) (54, 55), UniProt/SwissProt (April 28, 2016) (56), InterPro v.5.15.54 (57), and WormBase (*C. elegans* proteome in WS242) (58). To identify biologic pathways in *H. contortus* that were significantly affected after exposure to deguelin *in vitro*, differentially transcribed genes were subjected to enrichment by using the KEGG database employing a customised script in which Fisher's exact test was used to calculate *P* values. The R package

Pathview (v1.12.0) (59) was used to display enriched KEGG pathways.

Measuring the effects of deguelin on mitochondria within *H. contortus*

Oxygen consumption—representing oxidative phosphorylation—was measured in the medium surrounding *H. contortus* exsheathed L3s after exposure to varying concentrations (100, 50, 25, and 12.5 μM) of deguelin using the Seahorse XFe24 analyzer (Seahorse Biosciences, North Billerica, MA, USA), as previously described with minor modifications (60). In brief, exsheathed L3s were dispensed into XFe24 cell culture microplates (Seahorse Biosciences) at a density of ~600 exsheathed L3s per well in 600 μl of DMEM (Thermo Fisher Scientific) that was supplemented with 2 mM pyruvate and 2 mM glucose (pH 7.4). Four wells that contained Seahorse medium alone served as normalization controls. Deguelin was then dissolved in Seahorse medium, then loaded into the injection ports (in quadruplicate) and automatically dispensed into the XFe24 microplate after 5 measurements of respiration at intervals of 8 min. By using this approach, exsheathed L3s were exposed to final concentrations of deguelin of 100, 50, 25, 12.5, and 0 μM. Respiration rates were measured every 8 min for a period of 60 min, followed by measurements every 30 min for 15 h. To determine significant differences between treatments, the area under the curve was computed for each assay, and a nonparametric 1-way ANOVA using a Dunn's multiple comparison test was performed. A value of $P \leq 0.05$ was used (Prism v.7.01).

Mitochondria within exsheathed L3s of *H. contortus* were stained with tetramethylrhodamine ethyl ester (TMRE; Sigma-Aldrich, St. Louis, MO, USA), which is a cell-permeable, cationic, red-orange fluorescent dye that readily accumulates in active mitochondria because of their relative negative charge. Inactive mitochondria have limited membrane potential and do not sequester TMRE. Here, exsheathed L3s—prepared as in Procurement of *H. contortus*—were exposed (in triplicate) to 100, 50, 25, 12.5, 6.25, or 3.13 μM deguelin. Exsheathed L3s were also exposed (in triplicate) to the same concentrations of monepantel (nonmitochondrial inhibitor control). Untreated worms were exposed to 1% DMSO. After a 24-h incubation at 38°C and 10% CO_2, 1 μl TMRE (1:800) was added to each well and incubated for an additional 24 h. Before imaging worms, unbound TMRE was removed from the media by washing wells in the plate three times with 0.9% saline using a centrifuge with a plate insert (300 *g* for 5 min; 22–24°C). Worms were resuspended in 50 μl LB* and imaged by using a high-content imaging system (Operetta; PerkinElmer, Waltham, MA, USA). All experiments conducted to assess respiration and mitochondrial activity were repeated 3 times on separate days. Significant differences between treatments were determined by 1-way parametric ANOVA using a Holm-Sidak's multiple comparison test, setting a cutoff of $P \leq 0.05$.

Measuring the effect of deguelin on the free-living nematode *C. elegans*

The effect of deguelin on the mobility and the size of *C. elegans* was studied by using a microfluidic platform, as described previously (61), with slight modification. In brief, eggs of *C. elegans* (N2 wild-type strain; provided by the *Caenorhabditis* Genetics Center, University of Minnesota, Minneapolis, MN, USA) were hatched on solid nematode growth medium (NGM) agar plates that were seeded with *Escherichia coli* OP50, grown to L1, and injected into the microfluidic chip. Worms were fed a bacterial medium on chip (*E. coli* HT115 in complete S-medium) for a period of 20 h. After 20 h of feeding, deguelin at varying concentrations (1 mM, 100 μM, 10 μM, 1 μM, 100 nM, 10 nM, and 0 nM) was added to the medium and injected into the chip. After 42 h of treatment, a video recording and a picture were taken of each chamber, and the mobility and size of each worm in response to treatment was measured by using MovementTracker software (62). The fertility rates of worms were assessed at 64 h by manually counting the larvae and adult worms per chamber.

Oxygen consumption was also measured in *C. elegans* that were exposed to varying concentrations of deguelin by using the Seahorse XFe96 analyzer (63). In brief, eggs of *C. elegans* (N2 strain; provided by the *Caenorhabditis* Genetics Center, University of Minnesota) were hatched and grown to L4s on solid NGM plates using the OP50 strain of *E. coli* as a food source. L4s of *C. elegans* were then transferred from the NGM plates to wells of an XFe96 cell culture microplate, exposed to 1 mM, 100 μM, 10 μM, 1 μM, 100 nM, 10 nM, and 0 nM final concentrations of deguelin, and oxygen consumption was measured after 5 and 60 min of incubation. Worm paralysis was measured after 5 h by microscopically assessing the bending rate of *C. elegans* (63).

To measure the mitochondrial unfolded protein response (UPR^{mt}; 64), a microfluidic platform was used that employed the *hsp-6*:gfp transgenic strain of *C. elegans* (SJ4100 strain; provided by the *Caenorhabditis* Genetics Center, University of Minnesota). In brief, eggs of *hsp-6::gfp* worms were hatched on solid NGM agar plates that were seeded with *E. coli* OP50, grown to the L1 stage, and injected into the microfluidic chip. Worms were fed the bacterial medium on chip and treated with deguelin at varying concentrations (1 mM, 100 μM, 10 μM, 1 μM, 100 nM, 10 nM, and 0 nM). To measure the activation of UPR^{mt}, bright-field and fluorescent images were taken when the worm reached the adult stage (100 h) with and without deguelin treatment. Images were then measured for fluorescent intensity (GFP) using the software program ImageJ (NIH, Bethesda, MD, USA) as previously described (61). For all experiments, statistical analysis was conducted by using 1-way ANOVA, followed by a post Student's *t* test.

RESULTS

Screening results and the activity of deguelin on and selectivity for *H. contortus*

From the *in vitro* primary screening of the 260 natural compounds against *H. contortus*, only deguelin was found to reduce exsheathed L3 motility by ≥70% (**Fig. 1*A***). Deguelin was rescreened at 20 μM and shown to consistently inhibit exsheathed L3 motility. IC_{50} values for deguelin and those of reference anthelmintic compounds, monepantel and moxidectin (positive controls), on exsheathed L3 and L4 motility were determined at 24, 48, and 72 h, then compared. Although the monepantel and moxidectin control compounds were more effective than deguelin at inhibiting exsheathed L3s, with IC_{50} values of 1 ± 0.5, 1 ± 1.5 and 21 ± 0.7 μM, respectively (Fig. 1*B–D* and **Table 1**), deguelin was considerably more potent at inhibiting L4 motility at 72 h, with IC_{50} values of <0.004 μM compared with monepantel and moxidectin (IC_{50}: 3 ± 1.3 and 0.005 ± 0.53 μM, respectively; Fig. 1*F–H* and Table 1). In addition, after 72 h of exposure, deguelin was more potent at inhibiting L4 than exsheathed L3 motility. Deguelin was also shown to completely inhibit the development of L4s from exsheathed L3s at concentrations that ranged from 6.25 to 100 μM, with an IC_{50} value of 3.2 ± 0.04 μM (Fig. 1*E* and Table 1). Although deguelin was more potent at inhibiting L4 development than moxidectin

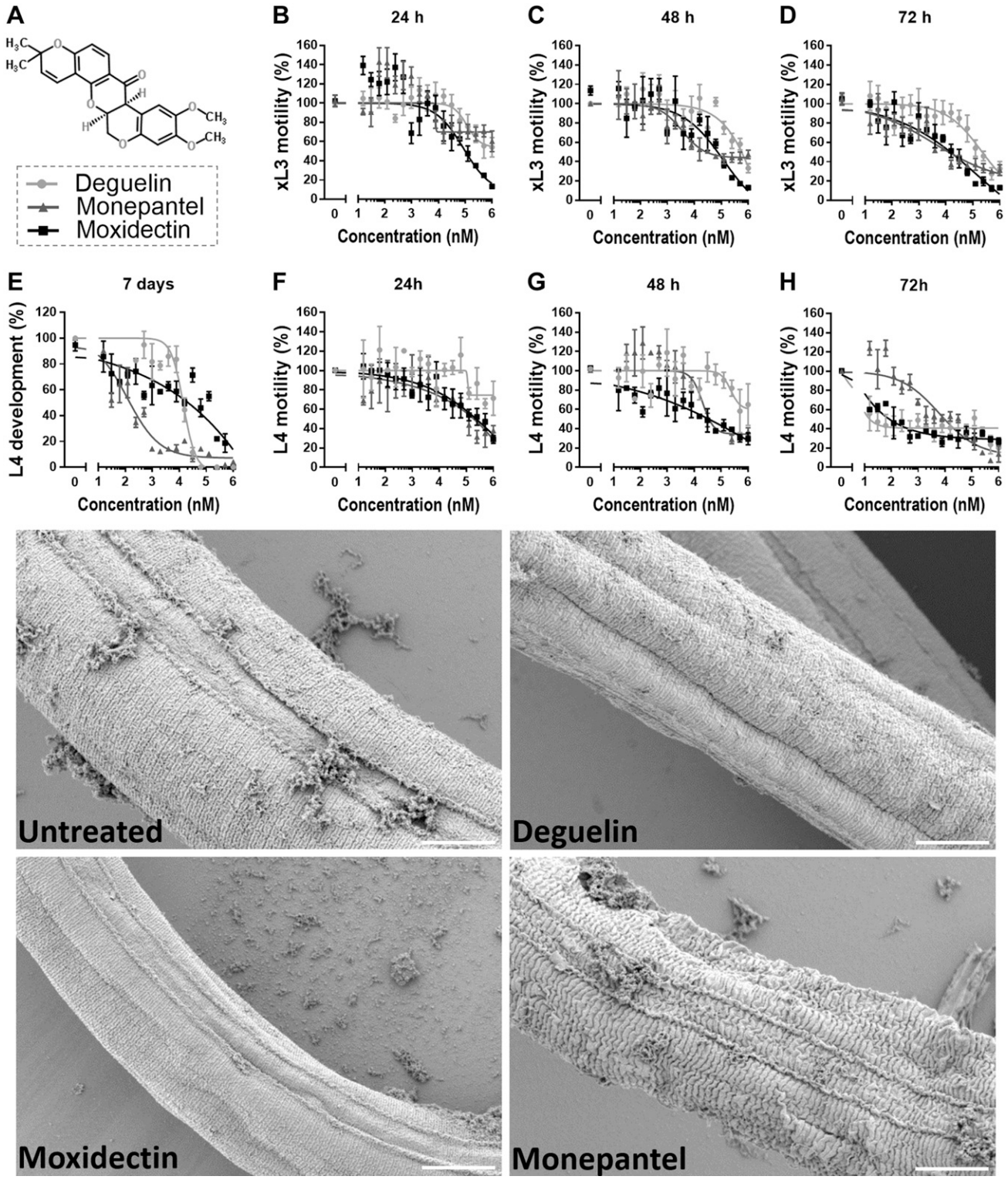

Figure 1. Activity of deguelin on the parasitic nematode *H. contortus* compared with reference compounds monepantel and moxidectin. *A*) The chemical structure of deguelin. (*B–H*) Dose response curves for deguelin and positive controls (monepantel and moxidectin) after a 24-, 48-, and 72-h incubation period on the motility of exsheathed L3 (xL3) and the motility and development of L4s. Bottom panels display representative scanning electron micrographs of L4s incubated with control medium (untreated control; LB plus 0.5% DMSO) or 100 μM of deguelin, monepantel, or moxidectin for 24 h. Scale bar, 5 μm.

(IC_{50}: 13.53 μM), it was less potent than monepantel (IC_{50}: 0.57 ± 0.55 μM). Deguelin was found to have low toxicity against NFFs by using a cell proliferation assay (IC_{50}: > 50 μM) with the greatest selectivity for *H. contortus vs.* NFFs observed for L4 motility (SI = 7143). In contrast, only modest selectivity was observed for L4 development (SI = 32) and only 2-fold selectivity for exsheathed L3s motility.

TABLE 1. Half maximum inhibitory concentrations (IC_{50}) of deguelin and the reference anthelmintic compounds monepantel and moxidectin on the motility and development of larval stages (exsheathed L3 and L4) of *H. contortus*

	Activity (IC_{50} values μM) against *H. contortus*						
	Exsheathed L3 motility			L4 motility			L4 development
Compound exposure time	24 h	48 h	72 h	24 h	48 h	72 h	7 d
Deguelin	81 ± 0.23	54 ± 3.10	21 ± 0.70	~11.39 ± 0.23	~25.4 ± 0.46	0.004 ± 0.80	3.2 ± 0.04
Monepantel	n.d.	7 ± 0.72	1 ± 0.50	4.3 ± 0.39	2.2 ± 0.77	3.0 ± 1.30	0.57 ± 0.55
Moxidectin	9 ± 0.46	5 ± 0.77	1 ± 1.50	2.2 ± 0.21	0.60 ± 0.20	0.005 ± 0.53	~13.53

IC_{50} values for deguelin, monepantel, and moxidectin were recorded at 24, 48, and 72 h (exsheathed L3 and L4 motility) and 7 d (L4 development). n.d., not detected; ~, indicates where IC_{50} values were estimated if the log(agonist) *vs.* response–variable slope (4 parameters) model could not be used to fit the curve.

Ultrastructural analysis of *H. contortus*

An SEM study of exsheathed L3s and L4s of *H. contortus* was undertaken. For exsheathed L3s, no morphologic difference was detected between deguelin-treated and untreated control worms (data not shown). This result is consistent with findings for monepantel and moxidectin, tested under the same conditions. In contrast, for L4s, deguelin-treatment resulted in longitudinal indentations of the cuticle, which were absent from untreated worms (Fig. 1, bottom). Monepantel was also shown to alter the morphology of L4s, which resulted in a perturbation of the cross-sectional striations of the cuticle and the formation of horizontal ridges and wrinkles; however, no detectable changes were evident on moxidectin-treated L4s (Fig. 1, bottom).

Analysis of transcription in *H. contortus* exsheathed L3s after exposure to deguelin

To begin to explore the molecular basis of how deguelin reduces motility and viability in *H. contortus*, we studied transcription in treated and untreated worms. First, we needed to identify an exposure time at which worms were expected to undergo considerable molecular alterations. To do this, exsheathed L3s were cultured *in vitro* in the presence or absence of 12.5 μM of deguelin for 72 h (4 biologic replicates), with exsheathed L3s motility assessed at 6, 24, 48, and 72 h (**Fig. 2*A***). The exposure of 30,000 exsheathed L3s to 12.5 μM deguelin resulted in a reduction of motility after 48 h (Fig. 2), which became significantly pronounced at 72 h (1.04 ± 0.06 compared with 0.6 ± 0.06; $P \leq 0.01$). In addition, at this time point (48 h), no L4 development had occurred in treated or untreated worms (Fig. 2*B*). The reduction in exsheathed L3 motility at 72 h was associated with a distinct, straight, and rigid phenotype, which did not develop to the L4 stage.

On the basis of this result, the 48-h time-point was selected (Fig. 2*A, B*) to capture a snapshot of changes in transcription in deguelin-treated exsheathed L3s, preceding the significant reduction in motility and L4 development after a 72-h deguelin exposure. The mRNA samples from 4 biologic replicates—each containing ~30,000 exsheathed L3s either treated or untreated for 48 h with 12.5 μM of deguelin—were subjected to RNA sequencing, followed by quality assessment and bioinformatic analyses.

After an assessment of the mapping of sequence reads from all replicates to the nonredundant transcriptome (63.5–65.7%; Supplemental Table 1), genes that were differentially transcribed between deguelin-treated and -untreated exsheathed L3s were identified by using edgeR (false discovery rate adjusted; $P \leq 0.01$). The 500 most highly up- or down-regulated genes were identified, clustered, and displayed in a heatmap (Fig. 2*C*). Of all 26,294 genes that were predicted to be encoded in the nonredundant transcriptome, 4052 (15%) were identified as differentially transcribed in response to deguelin treatment, 1813 genes were highly transcribed (up-regulated), and 2239 genes were lowly transcribed (down-regulated) relative to the untreated control (Fig. 2*D*). For differentially transcribed genes, the majority of up-regulated (87.2%) and down-regulated (86.4%) genes could be assigned at least 1 function *in silico* (Supplemental Table 2).

Protein families represented by up- and down-regulated genes after 48 h of exposure to deguelin

By using the KEGG BRITE functional hierarchy database, up- and down-regulated gene sets encoded proteins that could be classified into 40 and 38 unique functional groups (75–78% of all protein families in KEGG BRITE were represented among differentially transcribed genes; **Fig. 3** and Supplemental Tables 3 and 4). Of the up-regulated (annotated) transcripts, most (55.3%) encoded enzymes, such as hydrolases, transferases, and oxidoreductases, with ribosomal proteins (7.1%; mostly ribosomal proteins associated with the mitochondria), exosome components (4.4%), and mitochondrial biogenesis proteins (3.6%; mainly mitochondrial import machinery and mitochondrial DNA transcription, translation, and replication factors) also being prominently represented (Supplemental Table 3). Of the down-regulated (annotated) transcripts, approximately one half (50.7%) represented hydrolases, transferases, and oxidoreductases, with peptidases (5.6%), exosomal components (4.4%), and transport proteins (4.3%) also being represented (Supplemental Table 4). Specifically using the KEGG orthology classification within BRITE, most of the up-regulated annotated transcripts ($n = 719$) were associated with energy metabolism ($n = 353$; 49.1%) and genetic information and processing (specifically translation in the ribosome; $n = 227$; 31.6%;

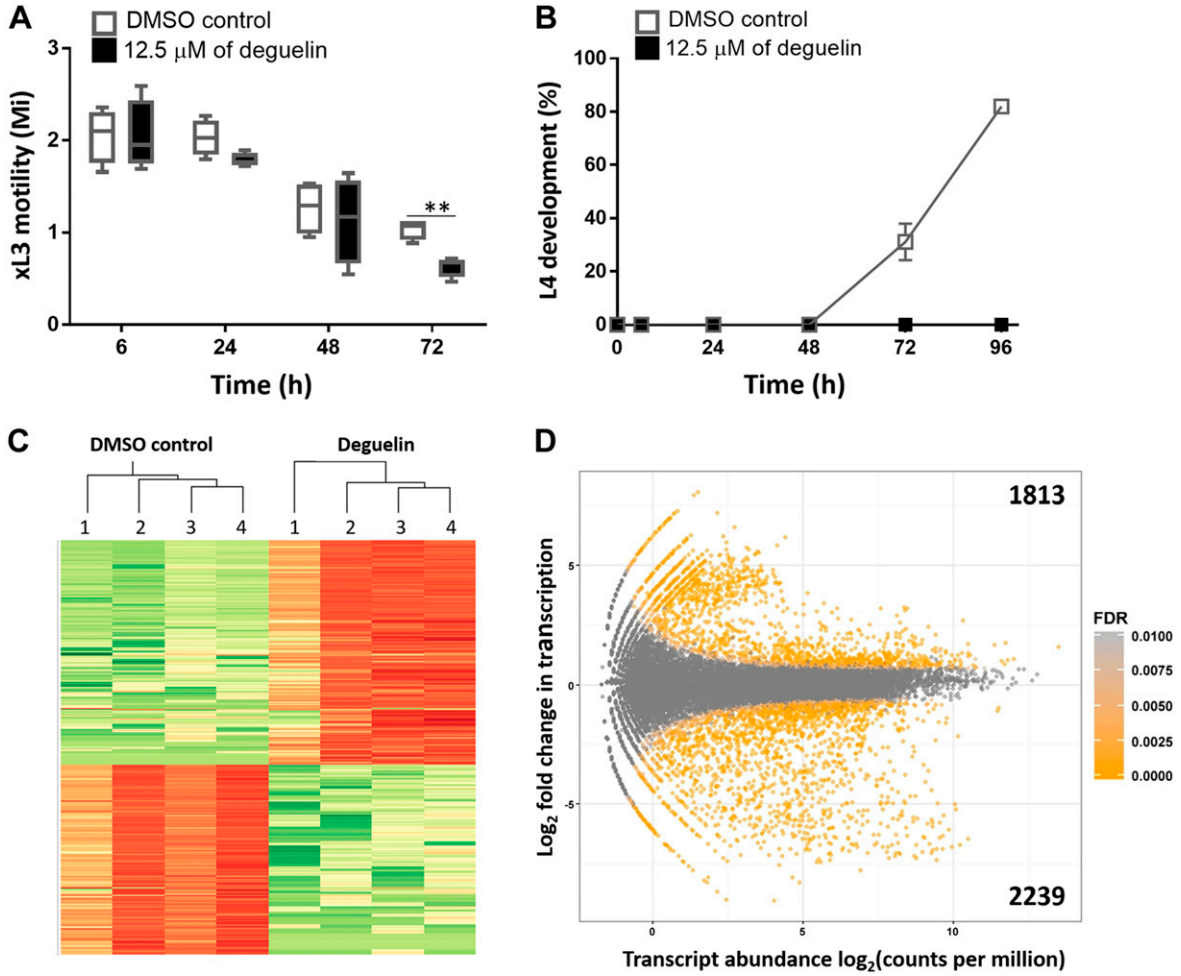

Figure 2. Transcriptomic analysis of exsheathed L3s *H. contortus* in response to deguelin treatment. *A*, *B*) The motility of exsheathed L3s and L4s development rate over time after treatment with 12.5 μM deguelin (black box) or matched DMSO control (clear box). $^{**}P < 0.01$. *C*) Heat map of the 500 most differentially transcribed genes in deguelin-treated worms and untreated controls, assayed in quadruplicate. Down-regulated genes are shown in shades of red; up-regulated genes in shades of green; replicates were clustered. *D*) Transcript abundance *vs.* change in transcription in deguelin-treated exsheathed L3s of *H. contortus* compared with untreated controls. Individual points represent transcripts and respective false discovery rate (FDR)–adjusted *P* values are indicated. Bold numbers indicate the number of transcripts which were up- or down-regulated in response to deguelin treatment. Mi, motility index.

Fig. 3 and Supplemental Table 3). In particular, of the energy metabolism pathways, oxidative phosphorylation was highly up-regulated in deguelin-treated exsheathed L3s compared with untreated larvae. Similarly, for genetic information and processing, genes that were associated with ribosomes were highly up-regulated. Other KEGG orthology protein families that were recorded to be up-regulated included those involved in xenobiotic biodegradation and metabolism, as well as those linked to bisphenol and polycyclic aromatic hydrocarbon degradation that involves enzymes such as esterases, lipases, and paraoxonases. Down-regulated annotated transcripts ($n = 573$) were linked to metabolism ($n = 197$; 34.4%), environmental information processing ($n = 125$; 21.8%), and cellular processes ($n = 83$; 14.5%; Fig. 3 and Supplemental Table 4). In particular, down-regulated were genes associated with the lysosome and signal transduction that is related to PI3K-Akt, Wnt, and Ras signaling (Fig. 3 and Supplemental Table 4).

Enrichment for up-regulated transcripts

The top 10 biologic pathways that were identified as highly enriched for up-regulated genes included those associated with oxidative phosphorylation and ribosomes, neurodegenerative disorders, and endocrine and metabolism disease, as well as the citric acid cycle (**Table 2**). In the oxidative phosphorylation pathway, highly up-regulated genes included those that encode the NADH dehydrogenase subunits (complex I), succinate dehydrogenase (complex II), cytochrome *c* reductase (complex III), cytochrome *c* oxidase (complex IV), and the ATP synthase proton pump (complex V; **Fig. 4*A***). Similarly, for pathways that have been inferred to be linked to neurodegenerative disorders, all showed substantial transcription pertaining to the oxidative phosphorylation pathway (complex I–V) as well as cytochrome *c* oxidase (Supplemental Table 3); high levels of transcription represented genes that encode mitochondrial membrane porin and

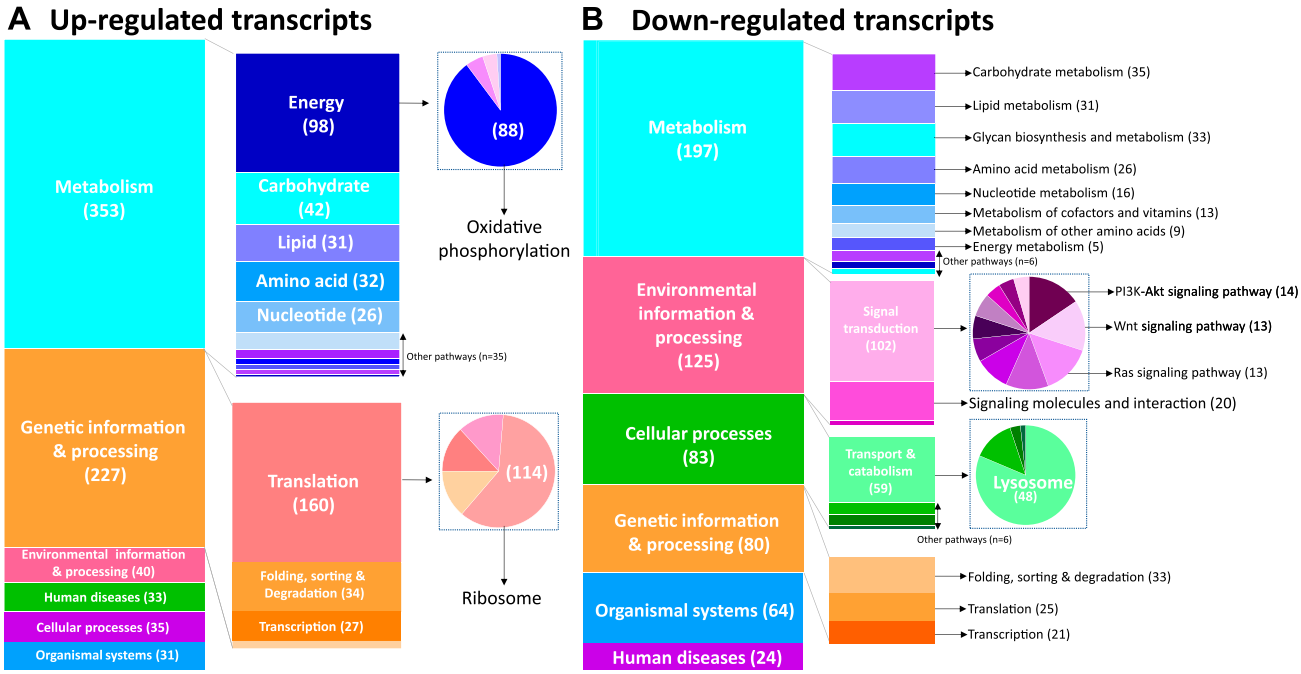

Figure 3. Graphical summary of the key KEGG orthology classification within BRITE affected by deguelin treatment. *A*, *B*) Up- and down-regulated protein families assigned by using the KEGG BRITE hierarchy database are summarized (drawn to scale). Numbers of transcripts representing particular KEGG pathways are in brackets. Shaded boxes have been drawn to scale to reflect the percent of transcripts in each category.

voltage-dependent anion channel protein 1 (Supplemental Table 3). In the ribosome pathway, genes that encode numerous ribosomal proteins that comprise the large and small subunits were highly up-regulated (Fig. 4*B*); many of the ribosomal proteins were of mitochondrial origin (62%; Supplemental Table 3). The remaining 3 pathways annotated represented metabolism, biosynthesis of amino acids, carbon metabolism, and the 2-oxocarboxylic acid pathway (Table 2 and Supplemental Table 3).

Enrichment for down-regulated transcripts

The top 10 biologic pathways that were identified as highly enriched for down-regulated genes included the lysosome pathway, represented by down-regulated genes that encode lysosomal acid hydrolases (cathepsins and legumain), glycosidases (glucuronidase-β and hexosaminidase), acid phosphatase 2, and such lysosomal membrane proteins as solute carriers and ATP pumps (**Fig. 5*A*** and Table 2). Genes that contribute to the suppression of metabolism were inferred to relate to carbohydrate metabolism, specifically amino sugar and nucleotide sugar metabolism (23% of genes), as well as fructose and mannose metabolism (20% of genes). Genes that were involved in sphingolipid metabolism and N-glycan biosynthesis were also down-regulated.

Three of the top 10 pathways were inferred to represent the immune system (antigen processing, presentation, and complement), coagulation cascades, and hematopoiesis (Table 2 and Supplemental Table 4). These findings were supported by a down-regulation of genes that encode cathepsins B and D, IFN-γ–inducible protein 30, legumain, tissue factor pathway inhibitor, thyroid peroxidase, neprilysin, platelet glycoprotein V, and aminopeptidase N. Pertaining to environmental information processing, the extracellular matrix–receptor interaction pathway was conspicuously suppressed on the basis of the finding of a down-regulation of genes that encode collagen, laminin, tenascin, and galactosyltransferases (Fig. 5*B*, Table 2, and Supplemental Table 4).

Effect of deguelin on nematode mitochondria in *H. contortus* and *C. elegans*

Mitochondrial activity measured by TMRE staining in *H. contortus* exsheathed L3s that were treated for 24 h with deguelin or monepantel was compared with that of untreated control worms (**Fig. 6*A***). Results indicated a significant decrease in mitochondrial activity in exsheathed L3s that were exposed to 100 and 50 μM of deguelin compared with untreated controls (62.5 ± 8.1 and 69.3 ± 6.8 *vs.* 94.4 ± 4.8; $P \leq 0.01$); however, exposure to less deguelin (25–12.5 μM) led to an increase in mitochondrial activity, with a significant increase being observed at 25 μM (127 ± 10.8 *vs.* 94.4 ± 4.8; $P \leq 0.05$; Fig. 6*A*). No change in mitochondrial activity was observed after exposure to monepantel (Fig. 6*B*). To measure the effect of deguelin on exsheathed L3s in real-time over 24 h, oxygen consumption—a measure of oxidative phosphorylation—was assayed. Similar to TMRE staining results, *H. contortus* exsheathed L3s that were exposed to 100 μM deguelin manifested an immediate reduction in oxygen consumption with reference to untreated control exsheathed L3s and a significant reduction in oxygen

TABLE 2. *The 10 most significantly up- and down-regulated pathways represented by differentially transcribed genes, annotated using the KEGG pathway database*

KEGG pathway annotation	KEGG pathway ID	Genes assigned to pathways, *n*	Total genes assigned to pathways, *n*	*P*
Up-regulated pathways				
Metabolism; energy metabolism; oxidative phosphorylation	ko00190	94	169	6.13×10^{-34}
Genetic information processing; translation; ribosome	ko03010	114	274	3.46×10^{-26}
Human diseases; neurodegenerative diseases; Huntington's disease	ko05016	80	174	9.64×10^{-22}
Human diseases; neurodegenerative diseases; Parkinson's disease	ko05012	77	142	7.70×10^{-27}
Human diseases; neurodegenerative diseases; Alzheimer's disease	ko05010	76	175	7.36×10^{-19}
Human diseases; endocrine and metabolic diseases; nonalcoholic fatty liver disease	ko04932	63	132	2.64×10^{-18}
Metabolism; carbohydrate metabolism; citric acid cycle	ko00020	33	62	8.72×10^{-12}
Metabolism; biosynthesis of amino acids	ko01230	43	106	5.81×10^{-10}
Metabolism; carbon metabolism	ko01200	49	134	2.50×10^{-09}
Metabolism; 2-oxocarboxylic acid metabolism	ko01210	18	32	1.74×10^{-07}
Down-regulated pathways				
Cellular processes; transport and catabolism; lysosome	ko04142	56	176	8.45×10^{-12}
Organismal systems; immune system; antigen processing and presentation	ko04612	22	53	1.21×10^{-07}
Environmental information processing; signaling molecules and interaction; ECM-receptor interaction	ko04512	19	51	6.17×10^{-06}
Organismal systems; immune system; complement and coagulation cascades	ko04610	7	9	1.43×10^{-05}
Organismal systems; immune system; hematopoietic cell lineage	ko04640	10	22	1.51×10^{-04}
Organismal systems; digestive system; protein digestion and absorption	ko04974	18	58	1.76×10^{-04}
Cellular processes; cell communication; adherens junction	ko04520	19	65	2.81×10^{-04}
Metabolism; glycan biosynthesis and metabolism; glycosphingolipid biosynthesis - globo series	ko00603	4	6	3.08×10^{-03}
Human diseases; immune diseases; autoimmune thyroid disease	ko05320	4	6	3.08×10^{-03}
Metabolism; glycan biosynthesis and metabolism; glycosphingolipid biosynthesis - lacto and neolacto series	ko00601	6	13	3.12×10^{-03}

Columns show the KEGG pathway annotation, pathway identification (ID) codes, number of differentially transcribed genes in one or more specific pathway, and the total number of genes assigned to particular pathways. Significance was determined by multiple Student's *t* tests and corrected for multiple comparisons. ECM, extracellular matrix.

consumption over the entire test period (107,816 ± 14,930 *vs.* 203,380 ± 31,869; $P \leq 0.05$; Fig. 6*C, D*). Exposed to 50–25 μM of deguelin, exsheathed L3s exhibited a gradual reduction in oxygen consumption over time (Fig. 6*C, D*).

Deguelin also substantially decreased oxygen consumption in *C. elegans* (Fig. 6*E*). Here, an almost complete inhibition of respiration was recorded after 5 min of exposure to 1 mM ($P < 0.001$), 100 μM ($P \leq 0.001$), and 10 μM ($P \leq 0.05$) of this chemical compared with untreated *C. elegans* (Fig. 6*F*). Similarly, oxygen consumption was significantly reduced 1 h after exposure to 1 mM ($P \leq 0.001$), 100 μM ($P \leq 0.001$), and 10 μM ($P \leq 0.001$) of deguelin compared with untreated *C. elegans* (Fig. 6*G*). In addition, L4s of *C. elegans* that were treated with 1 mM and 100 μM for 5 h were completely immobile, whereas at 10 and 1 μM, they exhibited a reduced bending rate (*i.e.*, increased paralysis) compared with untreated *C. elegans* (Fig. 6*H*). By using the microfluidic platform, deguelin was also shown to significantly decrease mobility, size, and fertility at concentrations of 10 μM, 100 μM, and 1 mM (**Fig. 7*B–D***). Given the hypothesis that deguelin exerts its potent effect on worm viability *via* the respiratory chain in the mitochondria, the unfolded protein response (UPR^{mt}), which is a marker of mitochondrial stress, was measured in transgenic *C. elegans*. After treatment with 10 and 100 μM of deguelin, UPR^{mt} was significantly activated, as indicated by the increase in *hsp-6::gfp* fluorescent signal compared with controls (Fig. 7*F*).

DISCUSSION

Natural products have been a source of medicines and remedies for millennia (65, 66). For example, rotenoids from plants of the family Leguminosae (6–10) are natural insecticides that are believed to target complex I of the electron transport chain (67, 68). The best known of the rotenoids are rotenone, tephrosine, toxicarol, and deguelin, which were patented collectively as insecticides in the

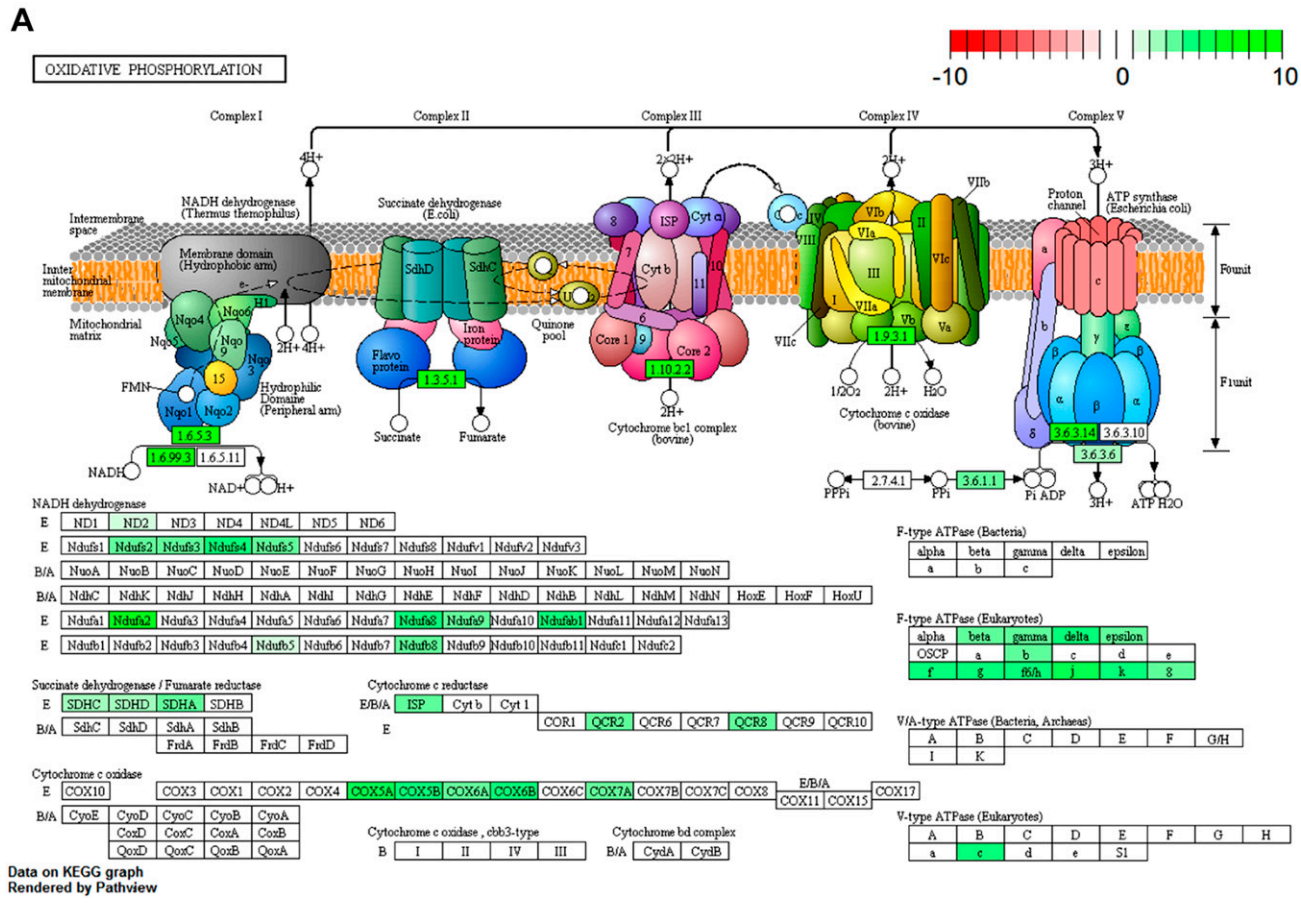

Figure 4. Graphical representation highlighting the genes involved in top 2 down-regulated pathways in exsheathed L3 *H. contortus* in response to deguelin treatment. *A*, *B*) Transcripts that encode protein subunits involved in oxidative phosphorylation (*A*) and ribosomal protein synthesis (*B*) are listed in individual boxes and shaded according to $\log_2$ (fold-change) in deguelin-treated exsheathed L3s relative to untreated controls. Scale bar indicates the relative expression of each gene, with shades of red indicating low transcription, and shades of green indicating high transcription compared with untreated control. Diagrams were produced by using the Pathview R package. a, archaea; b, bacteria; e, eukaryote.

1930s (Patent US2058832) (69). Particularly over the last 2 decades, there has been a considerable focus on studying deguelin as a chemopreventative, since the discovery of its antiproliferative properties on cells (70). These properties have been attributed to the modulation of myriad molecular pathways in various cancer cell types (6, 13, 17, 24–33), and the question arose as to whether deguelin might also have antiparasitic effects.

Here, by using a recently developed videographic assay (36, 37), we screened a natural product—small compound—library and identified deguelin as a potent inhibitor of motility and the development of parasitic larval stages (exsheathed L3s and L4s) of *H. contortus* and the free-living nematode (model organism) *C. elegans.* Deguelin also induced considerable cuticular damage to L4s upon short-term exposure and was shown to be selective for *H. contortus* over a mammalian fibroblast cell line. In addition, we demonstrated that deguelin inhibits the motility of nematodes *Trichostrongylus*, *Cooperia*, and *Ancylostoma* species *in vitro* (unpublished results), which are all related to *H. contortus* and *C. elegans*. To explore the molecular pathways that deguelin disrupts to inhibit both motility and development in *H. contortus*, we studied the transcriptional changes in protein-encoding genes in response to deguelin treatment. To do this, we elected to study the global changes in gene transcription in *H. contortus* exsheathed L3s in response to an intermediate concentration of deguelin. Specifically, we explored transcription 24 h before the significant decrease in motility after exposure to this chemical to identify biologic pathways that are affected early by deguelin as well as to prevent artifacts because of the possible degradation of RNA at later time points. Our analyses showed that genes up-regulated in response to deguelin are predominantly associated with energy metabolism, particularly oxidative phosphorylation, with drug-metabolism pathways also being activated, and that down-regulated genes were linked to aspects of parasite development and cuticle formation.

Notably, the most activated pathway in response to deguelin treatment was the oxidative phosphorylation pathway, which consists of the electron transport chain and is responsible for the production of ATP. A total of 94 genes were up-regulated, including genes that encode all 5 complexes of the electron transport chain. Only one gene in this pathway—encoding cytochrome *c* oxidase subunit 5b—was down-regulated. All other components were up-regulated in response to deguelin. Genes that are involved

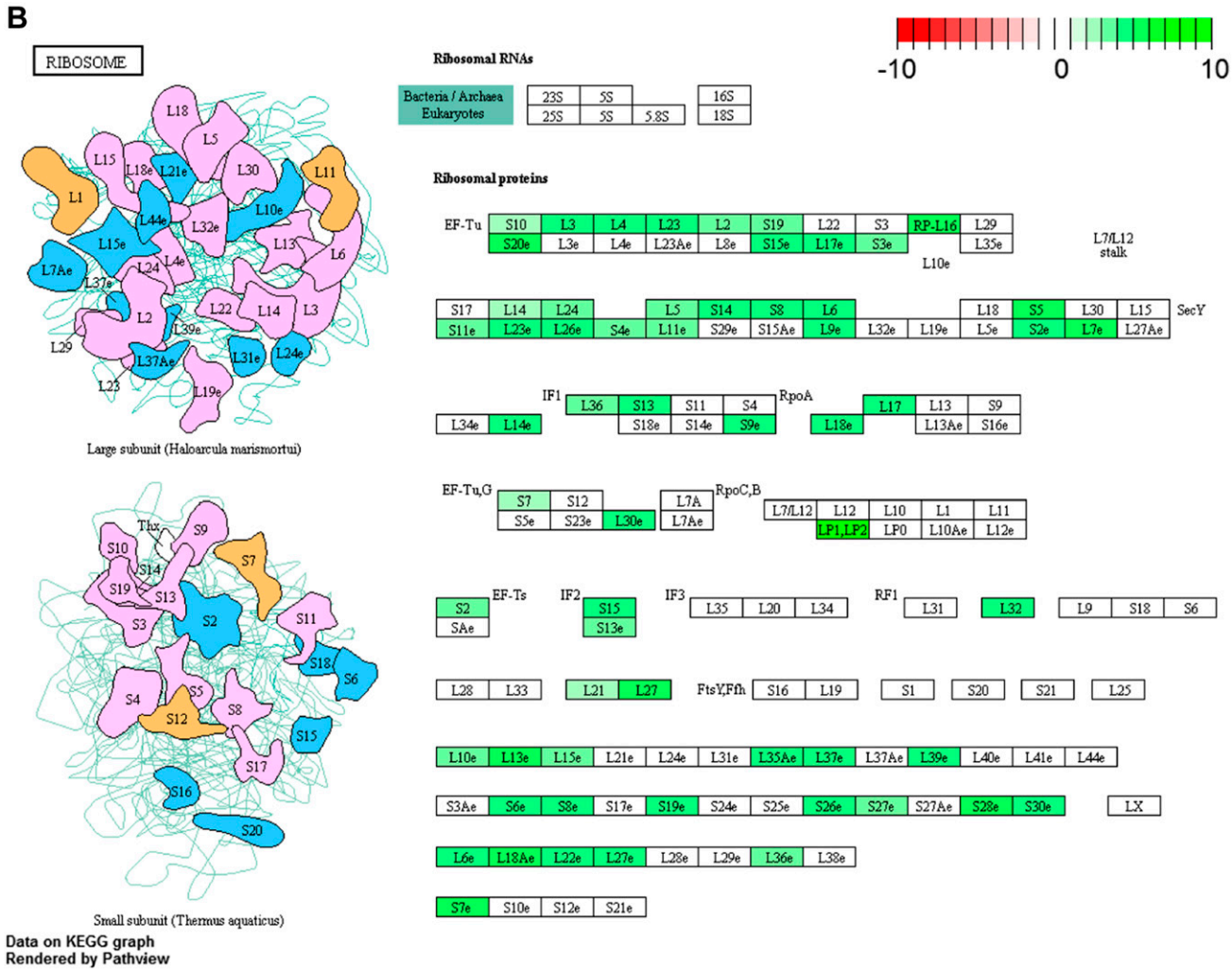

Figure 4. (*Continued*)

in the ribosome pathway were also highly transcribed, 62% of which encoded proteins located in the mito-ribosome. Mito-ribosomes synthesize proteins that are essential for oxidative phosphorylation and ATP synthesis (71), which suggests that exsheathed L3s of *H. contortus* have a substantial requirement for oxidative phosphorylation when exposed to deguelin and, by extension, that deguelin inhibits components of respiration.

It is generally accepted that free-living stages of parasitic helminths often depend heavily on aerobic respiration, whereas the parasitic stages depend more on anaerobic respiration as a result of limited access to oxygen inside the host animal (50, 72). Specifically, in hypoxic environments, adult parasitic nematodes rely on the phosphoenolpyruvate carboxykinase–succinate pathway to generate ATP (73, 74). This pathway is unique to organisms that live in environments with low oxygen tension, including some cancer cells, and is thus seen as a promising chemotherapeutic target (75–77); however, as *H. contortus* is a blood-feeding nematode and has access to a rich supply of oxygenated blood from its host, it is believed that this worm utilizes both aerobic and anaerobic respiratory pathways, which allows rapid adaption to the fluctuations in oxygen concentrations in its host (72).

Although most of the up-regulated pathways in deguelin-treated worms represent aerobic respiration, anaerobic pathways were also identified as being significantly up-regulated and associated with carbon fixation and glycolysis. On the basis of these findings and what is already known about the mode of action of deguelin in other organisms (6, 32, 33), we hypothesize that deguelin induces a loss in parasite viability, mainly by modulating or disrupting the function of the oxidative phosphorylation pathway, likely acting as a complex I inhibitor of the electron transport chain. Complex I is involved in both oxidative phosphorylation and the phosphoenolpyruvate carboxykinase–succinate pathway, which could account for the increased gene expression in both respiratory pathways. The proposal that deguelin is a complex I inhibitor in *H. contortus* is consistent with previous results for mammalian cells (6, 32, 33) and with the current observation of a substantial increase in transcription linked to energy metabolism–related pathways—that is, oxidative phosphorylation, citric acid cycle, mito-ribosomes biosynthesis, and glycolysis—24 h before a significant reduction in worm motility, most likely reflecting a compensatory/negative feedback response to the inhibition of complex I. We tested this hypothesis by using a

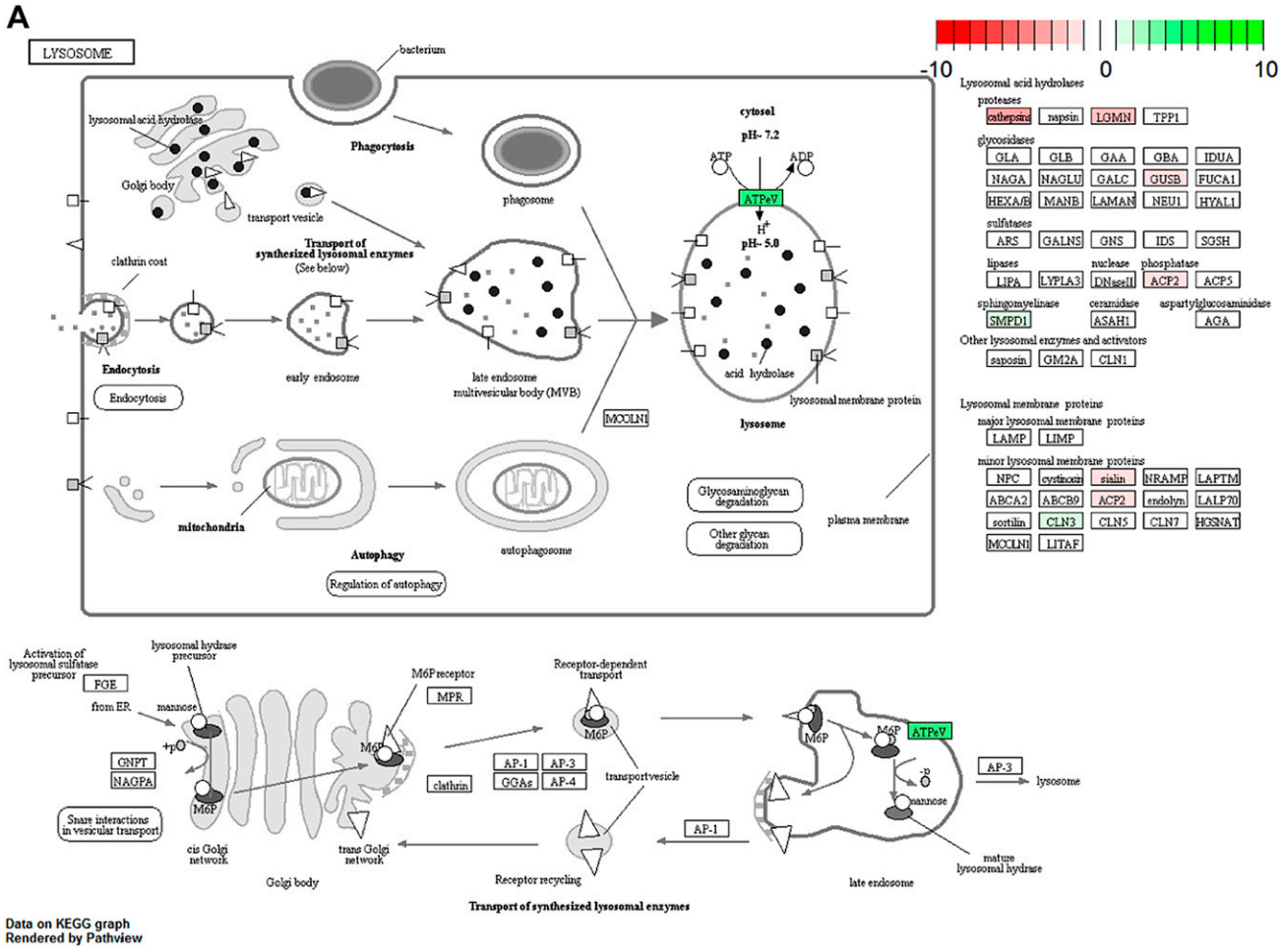

Figure 5. Graphical representation of genes involved in top 2 down-regulated pathways in exsheathed L3 *H. contortus* in response to deguelin treatment. *A*, *B*) Transcripts encoding protein subunits involved in lysosome (*A*) and extracellular matrix (ECM) receptor (*B*) pathways are listed in individual boxes and shaded according to $\log_2$ (fold-change) in deguelin-treated exsheathed L3s relative to untreated controls. Scale bar indicates the relative transcription of each gene, with shades of red indicating low transcription, and shades of green indicating high transcription compared with untreated control. Diagrams were produced using the Pathview R package.

fluorescent dye that is sequestered by active mitochondria and assessed mitochondrial activity in response to various concentrations of deguelin at 48 h. Here, exposure of *H. contortus* to high concentrations of deguelin ablated the activity of mitochondria, whereas low concentrations of deguelin increased their activity, which supports the RNA sequencing results.

To provide additional support for our hypothesis that deguelin acts as a complex I inhibitor to disrupt mitochondrial function, which results in a loss of parasite viability, oxidative phosphorylation was measured in exsheathed L3s in real time. Deguelin was shown to rapidly (after ~8 min) reduce oxygen consumption in *H. contortus* in a dose-dependent manner. This decrease preceded the inhibition of motility and development in this nematode, which indicates that this chemical decreases oxidative phosphorylation, leading—indirectly or directly—to a major reduction in larval motility and development. Recent studies have shown that inhibitors of oxidative phosphorylation can result in the activation of UPR^{mt} as a result of a mitonuclear protein imbalance (64). Given the high transcription of genes that encode mitochondrial ribosomal proteins in response to deguelin treatment, we examined the ability of deguelin to initiate UPR^{mt} in *C. elegans* and recorded this response in the presence of high concentrations of this chemical. UPR^{mt} is an evolutionary conserved stress response that is activated in normal physiologic and disease states to restore homeostasis (78). In *C. elegans*, UPR^{mt} is known to occur during the transition from L3 to L4 (79), where a burst of mitochondrial biogenesis occurs (80). During this transition, UPR^{mt} is relatively short-lived, but can be extended by perturbation by using pharmacologic and/or genetic mutations and has been associated with increased longevity (81). The finding that deguelin induces a phenotype in *C. elegans* that is similar to *H. contortus* provides a basis for gene knockdown experiments in *C. elegans* to confirm the target and down-stream signaling effects of deguelin treatment in parasitic nematodes. Such experiments would be extremely challenging to conduct in *H. contortus*.

Transcriptionally down-regulated genes in *H. contortus* in response to deguelin treatment were found to be predominantly involved in larval development and cuticle formation. Specifically, there was a down-regulation in the

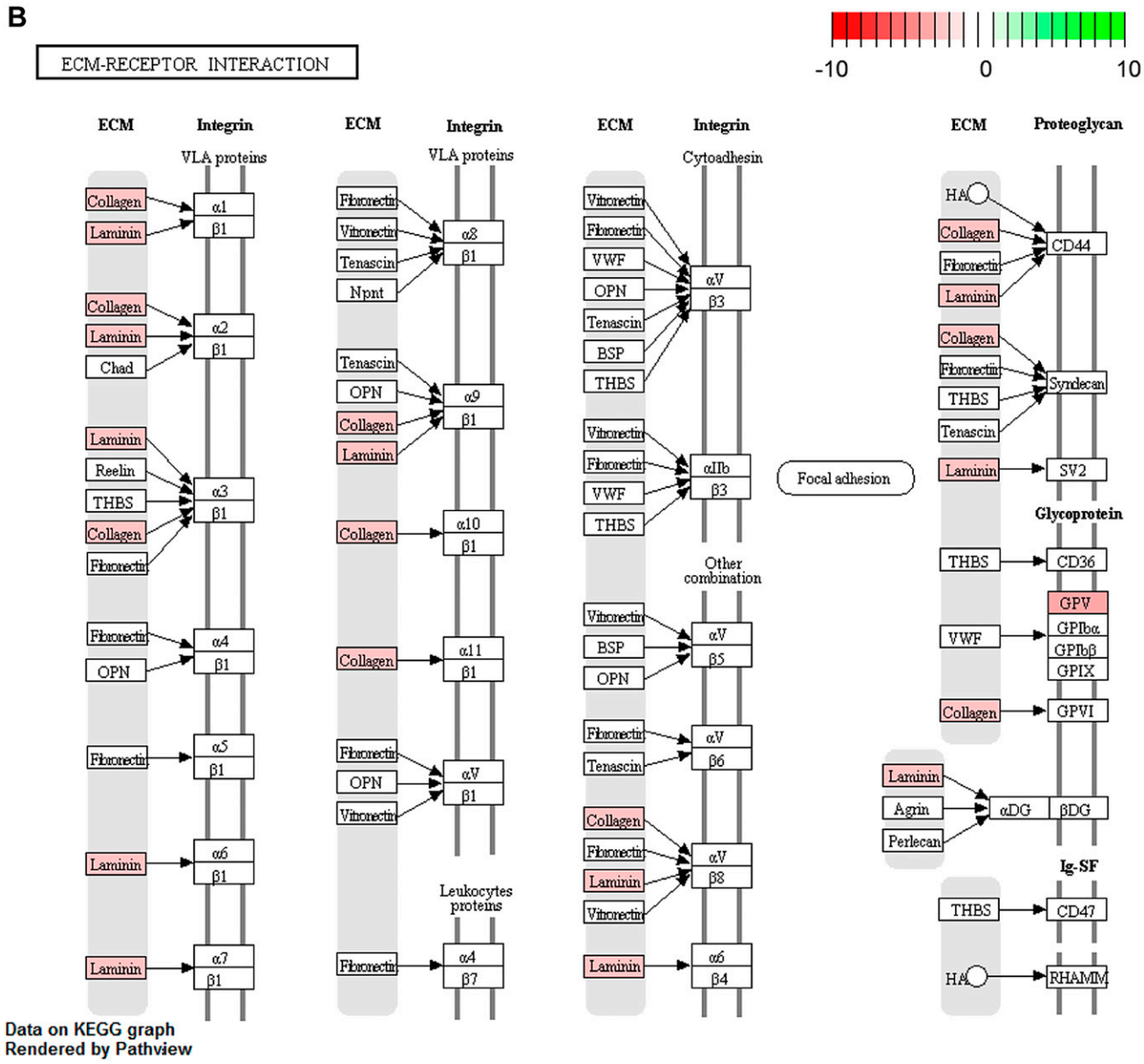

Figure 5. (*Continued*)

components of the lysosome, antigen-presenting and -processing pathways, as well as the extracellular matrix interaction pathway; all pathways link to genes that encode cysteine and aspartic peptidases, such as legumains and cathepsins, as well as the extracellular matrix interaction pathway, being mainly associated with proteins/enzymes, such as collagen, laminin, tenascin, and galactosyltransferases.

Legumains were originally identified in plants (82) but have since been found in many organisms, including such parasitic worms as *Schistosoma mansoni* and *Toxocara canis* (83, 84), and have been shown to or proposed to play roles in the digestion of host blood (85–87). Specifically, legumain is located on the microvillar surface of intestinal cells of *H. contortus*, and only in the blood-feeding stages of the parasite: L4 and adult (88). The location of legumain in the microvilli of intestinal cells coincides with that of the cysteine protease, cathepsins B (88, 89), and it has been proposed that legumain might activate cysteine proteases, such as cathepsins B and D (89). Cysteine peptidases, such as cathepsins, are well known for *H. contortus* and related strongylids as as result of their immune-protective properties (50, 90, 91). Cysteine proteases are highly abundant in excretory/secretory products and are involved in host digestion, immune evasion, nutrition acquisition, and cuticle molting in nematodes (92–94).

During molting in nematodes, cysteine proteases are released to breakdown the old cuticle (95–97). Cuticle components, such as collagen, tenascin, laminin, and galactosyltransferases (all required in the development of new cuticle) (94, 98, 99), were linked to genes with suppressed transcription upon deguelin exposure. Downregulation of genes that encode the structural proteins and key stage-specific enzymes supports the altered shape and structure of the cuticle as well as the inhibition of L4 development after *in vitro* exposure to deguelin. The

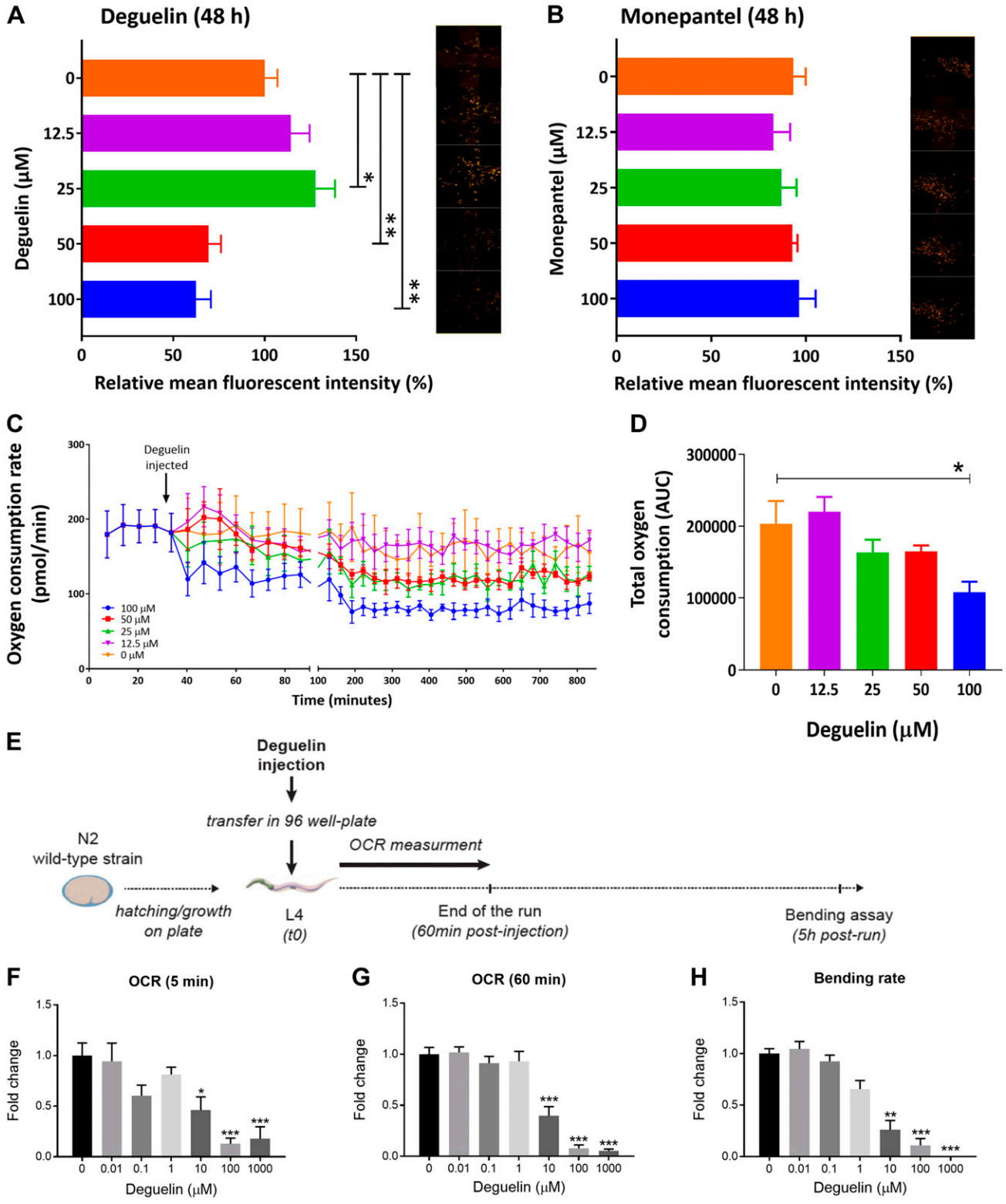

Figure 6. Effects of deguelin on mitochondrial activity in nematodes. *A*, *B*) Activity of *H. contortus* exsheathed L3s in response to treatment with various concentrations of deguelin or monepantel after a 48-h period. Mitochondrial activity was measured by a mitotracking stain (TMRE), and representative images for each treatment condition are shown adjacent to quantitative data. Data points represent means ± SEM from 3 independent assays. *C*) Kinetic profile of oxygen csonsumption in exsheathed L3s before and after exposure to deguelin (arrow) at various concentrations. Total oxygen consumption for each treatment group calculated from measuring the area under the curve (AUC) in panel *C. D)* Data in panels *C* and *D* represent means ± SEM from 4 biologic replicates. $*P \leq 0.05$. *E*) Schematic of the protocol for *C. elegans* experiments. *F*, *G*) An independent assessment of the effect of deguelin on the oxygen consumption rate (OCR) in *C. elegans* (a free-living nematode which is related to *H. contortus*) 5 and 60 min after treatment with deguelin. *H*) Dose-response curve showing the effect of deguelin on the bending rate of L4s of *C. elegans* after exposure to deguelin for 5 h. Data in panels *F*–*H* represent means ± SEM. $*P \leq 0.05$; $**P \leq 0.01$; $***P \leq 0.001$.

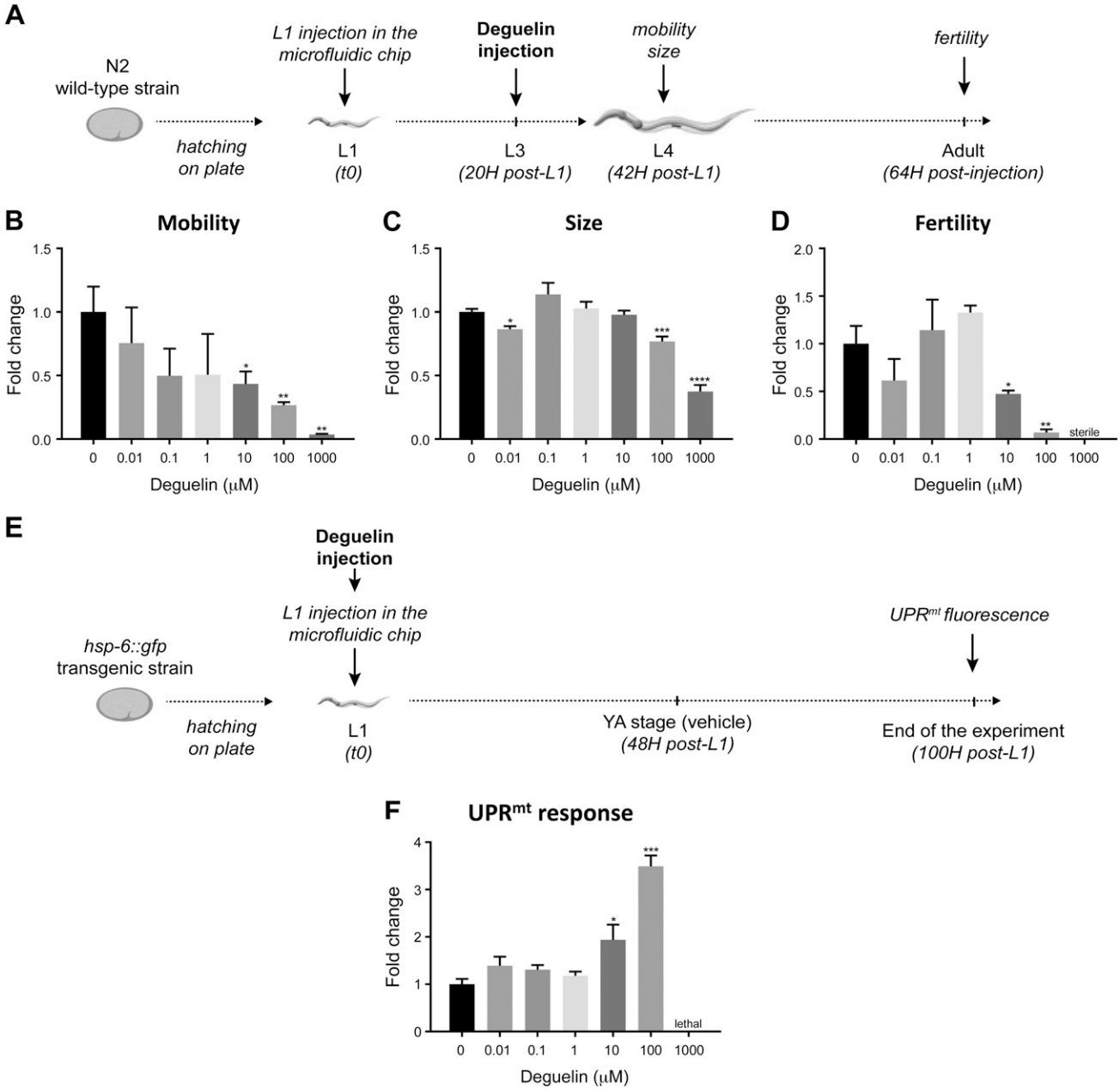

Figure 7. Assessing the effect of deguelin on *C. elegans* on the viability and UPR^{mt} in worms using the microfluidic platform. *A–D*) Schematic of the protocol (*A*) used to measure the effect of deguelin (1 mM, 100 μM, 10 μM, 1 μM, 100 nM, 10 nM, and 0 nM) on worm mobility, size, and fertility (*B–D*) using the microfluidic platform. *E*) Schematic of the protocol used to measure the effect of deguelin on the UPR^{mt} using the *hsp-6:gfp* transgenic strain of *C. elegans*. *F*) Activation of the UPR^{mt} in *C. elegans* after deguelin treatment at various concentrations (100 μM, 10 μM, 1 μM, 100 nM, 10 nM, and 0 nM). Data in panels *B–D* and *F* represent means ± SEM. $*P \leq 0.05$; $**P \leq 0.01$; $***P \leq 0.001$; $****P \leq 0.0001$. YA, young adult.

nematode cuticle predominantly consists of cross-linked collagens and coated with an external layer of lipids and glycoproteins, such that changes in the transcription or function of genes associated with these components can severely alter body shape, molting, and/or viability of nematodes (100–102). It is not clear whether the transcriptional down-regulation of these genes is a direct or indirect response to deguelin exposure and should be a subject for additional investigation. Finally, of interest was the suppression of genes that are involved in the PI3K-Akt kinase signaling pathway (represented by 13 genes), which has been identified as a target of deguelin in mammalian cells (24–26). Recently, this pathway was shown to modulate oxygen metabolism *via* phosphorylation of pyruvate dehydrogenase (103). Additional experimental work will be required to understand the link between the PI3K-Akt kinase signaling pathway and oxygen metabolism in *H. contortus* and its relationship with deguelin.

Overall analyses of transcriptional responses to deguelin, together with mitochondrial biologic information, have revealed a clear modulation of energy metabolism in *H. contortus*. Integration of biologic and molecular data sets points to complex I of the electron transport chain being a target for deguelin in *H. contortus* and *C. elegans*.

Given the toxicity of deguelin on *C. elegans*, loss of function studies in this model organism would aid in identifying and proving the target of deguelin in nematodes. Although not essential for drug discovery and development, understanding the mode of action of a drug on a target organism will aid in predicting aspects of host toxicity, adverse effects, and/or potential modes of drug resistance (104). FJ

ACKNOWLEDGMENTS

This study was supported by the Australian Research Council and the National Health and Medical Research Council (NHMRC) of Australia, as well as by the Medicines for Malaria Venture, Yourgene Bioscience, the University of Melbourne (to R.B.G. S.P., A.J., J.B., B.C.H.C., and A.H.), the École Polytechnique Fédérale de Lausanne, and the Gebert Rüf Stiftung (GRS-025/16) and the AgingX program of the Swiss Initiative for Systems Biology (to J.A. and L.H.). Some work was supported by the EU Ideas Program (ERC-2012-AdG-320404; to M.A.M.G and M.C.). G.M.F. was supported by a postdoctoral fellowship and a new researcher grant from Griffith University. P.K.K. was supported by an early career research fellowship, and N.D.Y. by a career development fellowship (CDF1) from NHMRC. Funding bodies played no role in the design of the study or collection, analysis, or interpretation of data, or in the writing of the manuscript. The authors thank Compounds Australia (*http://www.griffith.edu.au/science-aviation/compounds-australia*) for access to the Davis open-access natural product library, which forms part of the Open Access Compound Collection. The authors declare no conflicts of interest.

AUTHOR CONTRIBUTIONS

S. Preston, L. Mouchiroud, S. L. McGee, K. T. Andrews, B. Chang, M. A. M. Gijs, P. W. Sternberg, J. Auwerx, J. Baell, A. Hofmann, A. Jabbar, and R. B. Gasser designed research; S. Preston, P. K. Korhonen, L. Mouchiroud, M. Cornaglia, and B. R. E. Ansell analyzed data; S. Preston, L. Mouchiroud, M. Cornaglia, S. L. McGee, N. D. Young, S. Crawford, and G. M. Fisher performed research; S. Preston, L. Mouchiroud, and R. B. Gasser wrote the paper; R. A. Davis contributed reagents; and C. Nowell developed software to analyze data.

REFERENCES

1. Epe, C., and Kaminsky, R. (2013) New advancement in anthelmintic drugs in veterinary medicine. *Trends Parasitol.* **29**, 129–134
2. Shen, B. (2015) A new golden age of natural products drug discovery. *Cell* **163**, 1297–1300
3. Newman, D. J., and Cragg, G. M. (2012) Natural products as sources of new drugs over the 30 years from 1981 to 2010. *J. Nat. Prod.* **75**, 311–335
4. Eder, J., Sedrani, R., and Wiesmann, C. (2014). The discovery of first-in-class drugs: origins and evolution. *Nat. Rev. Drug Disc.* **13**, 577–587
5. Baell, J. B. (2016) Feeling nature's pains: natural products, natural product drugs, and pan assay interference compounds (PAINS). *J. Nat. Prod.* **79**, 616–628
6. Fang, N., and Casida, J. E. (1998) Anticancer action of cubé insecticide: correlation for rotenoid constituents between inhibition of NADH:ubiquinone oxidoreductase and induced ornithine decarboxylase activities. *Proc. Natl. Acad. Sci. USA* **95**, 3380–3384
7. Cabizza, M., Angioni, A., Melis, M., Cabras, M., Tuberoso, C. V., and Cabras, P. (2004) Rotenone and rotenoids in cubè resins, formulations, and residues on olives. *J. Agric. Food Chem.* **52**, 288–293
8. Wenjie, J., Yuchun, F., Chunji, G., Yunhui, W., and Pang, J. (2009) Extraction and purification of deguelin from *Derris trifoliata* Lour root. *Int. J. Agric. Biol. Eng.* **2**, 98–103
9. Chen, C. S., Ho, D. R., Chen, F. Y., Chen, C. R., Ke, Y. D., and Su, J. G. J. (2014) AKT mediates actinomycin D-induced p53 expression. *Oncotarget* **5**, 693–703
10. Vats, S., and Kamal, R. (2014) *Cassia occidentalis L.* (a new source of rotenoids): its *in vitro* regulation by feeding precursors and larvicidal efficacy. *Plant Cell Tissue Organ Cult.* **116**, 403–409
11. Ashack, R. J., McCarty, L. P., Malek, R. S., Goodman, F. R., and Peet, N. P. (1980) Evaluation of rotenone and related compounds as antagonists of slow-reacting substance of anaphylaxis. *J. Med. Chem.* **23**, 1022–1026
12. Okombe Embeya, V., Lumbu Simbi, J. B., Stévigny, C., Vandenput, S., Pongombo Shongo, C., and Duez, P. (2014) Traditional plant-based remedies to control gastrointestinal disorders in livestock in the regions of Kamina and Kaniama (Katanga province, Democratic Republic of Congo). *J. Ethnopharmacol.* **153**, 686–693
13. Gerhauser, C., Lee, S. K., Kosmeder, J. W., Moriarty, R. M., Hamel, E., Mehta, R. G., Moon, R. C., and Pezzuto, J. M. (1997) Regulation of ornithine decarboxylase induction by deguelin, a natural product cancer chemopreventive agent. *Cancer Res.* **57**, 3429–3435
14. Udeani, G. O., Gerhauser, C., Thomas, C. F., Moon, R. C., Kosmeder, J. W., Kinghorn, A. D., Moriarty, R. M., and Pezzuto, J. M. (1997) Cancer chemopreventive activity mediated by deguelin, a naturally occurring rotenoid. *Cancer Res.* **57**, 3424–3428
15. Lee, H. Y., Oh, S. H., Woo, J. K., Kim, W. Y., Van Pelt, C. S., Price, R. E., Cody, D., Tran, H., Pezzuto, J. M., Moriarty, R. M., and Hong, W. K. (2005) Chemopreventive effects of deguelin, a novel Akt inhibitor, on tobacco-induced lung tumorigenesis. *J. Natl. Cancer Inst.* **97**, 1695–1699
16. Arulampalam, V., Kolosenko, I., Hjortsberg, L., Björklund, A. C., Grandér, D., and Tamm, K. P. (2011) Activation of STAT1 is required for interferon-alpha-mediated cell death. *Exp. Cell Res.* **317**, 9–19
17. Boreddy, S. R., and Srivastava, S. K. (2013) Deguelin suppresses pancreatic tumor growth and metastasis by inhibiting epithelial-to-mesenchymal transition in an orthotopic model. *Oncogene* **32**, 3980–3991
18. Farmer, R. L., and Scheidt, K. A. (2013) A concise enantioselective synthesis and cytotoxic evaluation of the anticancer rotenoid deguelin enabled by a tandem knoevenagel/conjugate addition/decarboxylation sequence. *Chem. Sci.* **4**, 3304–3309
19. Shang, H. S., Chang, J. B., Lin, J. H., Lin, J. P., Hsu, S. C., Liu, C. M., Liu, J. Y., Wu, P. P., Lu, H. F., Au, M. K., and Chung, J. G. (2014) Deguelin inhibits the migration and invasion of U-2 OS human osteosarcoma cells *via* the inhibition of matrix metalloproteinase-2/-9 *in vitro*. *Molecules* **19**, 16588–16608
20. Lee, H. Y. (2004) Molecular mechanisms of deguelin-induced apoptosis in transformed human bronchial epithelial cells. *Biochem. Pharmacol.* **68**, 1119–1124
21. Paulus, P., Ockelmann, P., Tacke, S., Karnowski, N., Ellinghaus, P., Scheller, B., Holfeld, J., Urbschat, A., and Zacharowski, K. (2012) Deguelin attenuates reperfusion injury and improves outcome after orthotopic lung transplantation in the rat. *PLoS One* **7**, e39265
22. Caboni, P., Sherer, T. B., Zhang, N., Taylor, G., Na, H. M., Greenamyre, J. T., and Casida, J. E. (2004) Rotenone, deguelin, their metabolites, and the rat model of Parkinson's disease. *Chem. Res. Toxicol.* **17**, 1540–1548
23. Udeani, G. O., Zhao, G. M., Shin, Y. G., Kosmeder II, J. W., Beecher, C. W., Kinghorn, A. D., Moriarty, R. M., Moon, R. C., and Pezzuto, J. M. (2001) Pharmacokinetics of deguelin, a cancer chemopreventive agent in rats. *Cancer Chemother. Pharmacol.* **47**, 263–268
24. Mehta, R., Katta, H., Alimirah, F., Patel, R., Murillo, G., Peng, X., Muzzio, M., and Mehta, R. G. (2013) Deguelin action involves c-Met and EGFR signaling pathways in triple negative breast cancer cells. *PLoS One* **8**, e65113
25. Bortul, R., Tazzari, P. L., Billi, A. M., Tabellini, G., Mantovani, I., Cappellini, A., Grafone, T., Martinelli, G., Conte, R., and Martelli, A. M. (2005) Deguelin, A PI3K/AKT inhibitor, enhances chemosensitivity of leukaemia cells with an active PI3K/AKT pathway. *Br. J. Haematol.* **129**, 677–686
26. Wu, W., Hai, Y., Chen, L., Liu, R. J., Han, Y. X., Li, W. H., Li, S., Lin, S., and Wu, X. R. (2016) Deguelin-induced blockade of PI3K/protein kinase B/MAP kinase signaling in zebrafish and breast cancer cell lines is mediated by down-regulation of fibroblast growth factor receptor 4 activity. *Pharmacol. Res. Perspect.* **4**, e00212
27. Kim, W. Y., Chang, D. J., Hennessy, B., Kang, H. J., Yoo, J., Han, S. H., Kim, Y. S., Park, H. J., Seo, S. Y., Mills, G., Kim, K. W., Hong, W. K.,

Suh, Y. G., and Lee, H. Y. (2008) A novel derivative of the natural agent deguelin for cancer chemoprevention and therapy. *Cancer Prev. Res.* **1**, 577–587
28. Suh, Y. A., Kim, J. H., Sung, M. A., Boo, H. J., Yun, H. J., Lee, S. H., Lee, H. J., Min, H. Y., Suh, Y. G., Kim, K. W., and Lee, H. Y. (2013) A novel antitumor activity of deguelin targeting the insulin-like growth factor (IGF) receptor pathway *via* up-regulation of IGF-binding protein-3 expression in breast cancer. *Cancer Lett.* **332**, 102–109
29. Lee, S. C., Min, H. Y., Choi, H., Kim, H. S., Kim, K. C., Park, S. J., Seong, M. A., Seo, J. H., Park, H. J., Suh, Y. G., Kim, K. W., Hong, H. S., Kim, H., Lee, M. Y., Lee, J., and Lee, H. Y. (2015) Synthesis and evaluation of a novel deguelin derivative, L80, which disrupts ATP binding to the C-terminal domain of heat shock protein 90. *Mol. Pharmacol.* **88**, 245–255
30. Thamilselvan, V., Menon, M., and Thamilselvan, S. (2011) Anticancer efficacy of deguelin in human prostate cancer cells targeting glycogen synthase kinase-3 β/β-catenin pathway. *Int. J. Cancer* **129**, 2916–2927
31. Liu, Y. P., Lee, J. J., Lai, T. C., Lee, C. H., Hsiao, Y. W., Chen, P. S., Liu, W. T., Hong, C. Y., Lin, S. K., Ping Kuo, M. Y., Lu, P. J., and Hsiao, M. (2016) Suppressive function of low-dose deguelin on the invasion of oral cancer cells by downregulating tumor necrosis factor alpha-induced nuclear factor-kappa B signaling. *Head Neck* **38** (Suppl 1), E524–E534
32. Garcia, J., Barluenga, S., Gorska, K., Sasse, F., and Winssinger, N. (2012) Synthesis of deguelin-biotin conjugates and investigation into deguelin's interactions. *Bioorg. Med. Chem.* **20**, 672–680
33. Vrana, J. A., Boggs, N., Currie, H. N., and Boyd, J. (2013) Amelioration of an undesired action of deguelin. *Toxicon* **74**, 83–91
34. Chang, D. J., An, H., Kim, K. S., Kim, H. H., Jung, J., Lee, J. M., Kim, N. J., Han, Y. T., Yun, H., Lee, S., Lee, G., Lee, S., Lee, J. S., Cha, J. H., Park, J. H., Park, J. W., Lee, S. C., Kim, S. G., Kim, J. H., Lee, H. Y., Kim, K. W., and Suh, Y. G. (2012) Design, synthesis, and biological evaluation of novel deguelin-based heat shock protein 90 (HSP90) inhibitors targeting proliferation and angiogenesis. *J. Med. Chem.* **55**, 10863–10884
35. Lee, S. C., Min, H. Y., Choi, H., Bae, S. Y., Park, K. H., Hyun, S. Y., Lee, H. J., Moon, J., Park, S. H., Kim, J. Y., An, H., Park, S. J., Seo, J. H., Lee, S., Kim, Y. M., Park, H. J., Lee, S. K., Lee, J., Lee, J., Kim, K. W., Suh, Y. G., and Lee, H. Y. (2016) Deguelin analogue SH-1242 inhibits Hsp90 activity and exerts potent anticancer efficacy with limited neurotoxicity. *Cancer Res.* **76**, 686–699
36. Preston, S., Jabbar, A., Nowell, C., Joachim, A., Ruttkowski, B., Baell, J., Cardno, T., Korhonen, P. K., Piedrafita, D., Ansell, B. R. E., Jex, A. R., Hofmann, A., and Gasser, R. B. (2015) Low cost whole-organism screening of compounds for anthelmintic activity. *Int. J. Parasitol.* **45**, 333–343
37. Preston, S., Jabbar, A., Nowell, C., Joachim, A., Ruttkowski, B., Cardno, T., Hofmann, A., and Gasser, R. B. (2016) Practical and low cost whole-organism motility assay: a step-by-step protocol. *Mol. Cell. Probes* **30**, 13–17
38. Davis, R. A. (2005) Isolation and structure elucidation of the new fungal metabolite (−)-xylariamide A. *J. Nat. Prod.* **68**, 769–772
39. Barnes, E. C., Said, N. A. B. M., Williams, E. D., Hooper, J. N. A., and Davis, R. A. (2010) Ecionines A and B, two new cytotoxic pyridoacridine alkaloids from the Australian marine sponge, *Ecionemia geodides*. *Tetrahedron* **66**, 283–287
40. Levrier, C., Balastrier, M., Beattie, K. D., Carroll, A. R., Martin, F., Choomuenwai, V., and Davis, R. A. (2013) Pyridocoumarin, aristolactam and aporphine alkaloids from the Australian rainforest plant *Goniothalamus australis*. *Phytochemistry* **86**, 121–126
41. Barnes, E. C., Kumar, R., and Davis, R. A. (2016) The use of isolated natural products as scaffolds for the generation of chemically diverse screening libraries for drug discovery. *Nat. Prod. Rep.* **33**, 372–381
42. Fisher, G. M., Tanpure, R. P., Douchez, A., Andrews, K. T., and Poulsen, S. A. (2014) Synthesis and evaluation of antimalarial properties of novel 4-aminoquinoline hybrid compounds. *Chem. Biol. Drug Des.* **84**, 462–472
43. Preston, S., Luo, J., Zhang, Y., Jabbar, A., Crawford, S., Baell, J., Hofmann, A., Hu, M., Zhou, H. B., and Gasser, R. B. (2016) Selenophene and thiophene-core estrogen receptor ligands that inhibit motility and development of parasitic stages of *Haemonchus contortus*. *Parasit. Vectors* **9**, 346
44. Korhonen, P. K., Pozio, E., La Rosa, G., Chang, B. C. H., Koehler, A. V., Hoberg, E. P., Boag, P. R., Tan, P., Jex, A. R., Hofmann, A., Sternberg, P. W., Young, N. D., and Gasser, R. B. (2016) Phylogenomic and biogeographic reconstruction of the *Trichinella* complex. *Nat. Commun.* **7**, 10513
45. Bolger, A. M., Lohse, M., and Usadel, B. (2014) Trimmomatic: a flexible trimmer for Illumina sequence data. *Bioinformatics* **30**, 2114–2120
46. Zerbino, D. R., and Birney, E. (2008) Velvet: algorithms for *de novo* short read assembly using de Bruijn graphs. *Genome Res.* **18**, 821–829
47. Schulz, M. H., Zerbino, D. R., Vingron, M., and Birney, E. (2012) Oases: robust *de novo* RNA-seq assembly across the dynamic range of expression levels. *Bioinformatics* **28**, 1086–1092
48. Li, W., and Godzik, A. (2006) Cd-hit: a fast program for clustering and comparing large sets of protein or nucleotide sequences. *Bioinformatics* **22**, 1658–1659
49. Mount, D. W. (2007) *Using the Basic Local Alignment Search Tool (BLAST)*, Cold Spring Harbor Protocols, Cold Spring Harbor, NY
50. Schwarz, E. M., Korhonen, P. K., Campbell, B. E., Young, N. D., Jex, A. R., Jabbar, A., Hall, R. S., Mondal, A., Howe, A. C., Pell, J., Hofmann, A., Boag, P. R., Zhu, X. Q., Gregory, T., Loukas, A., Williams, B. A., Antoshechkin, I., Brown, C., Sternberg, P. W., and Gasser, R. B. (2013) The genome and developmental transcriptome of the strongylid nematode *Haemonchus contortus*. *Genome Biol.* **14**, R89
51. Li, B., and Dewey, C. N. (2011) RSEM: accurate transcript quantification from RNA-Seq data with or without a reference genome. *BMC Bioinformatics* **12**, 323
52. Robinson, M. D., McCarthy, D. J., and Smyth, G. K. (2010) edgeR: a bioconductor package for differential expression analysis of digital gene expression data. *Bioinformatics* **26**, 139–140
53. Pruitt, K. D., Tatusova, T., Brown, G. R., and Maglott, D. R. (2012) NCBI reference sequences (RefSeq): current status, new features and genome annotation policy. *Nucleic Acids Res.* **40**, D130–D135
54. Kanehisa, M., and Goto, S. (2000) KEGG: Kyoto Encyclopedia of Genes and Genomes. *Nucleic Acids Res.* **28**, 27–30
55. Kanehisa, M., Goto, S., Sato, Y., Furumichi, M., and Tanabe, M. (2012) KEGG for integration and interpretation of large-scale molecular data sets. *Nucleic Acids Res.* **40**, D109–D114
56. Magrane, M.; UniProt Consortium. (2011) UniProt knowledgebase: a hub of integrated protein data. *Database (Oxford)* **2011**, bar009
57. Hunter, S., Jones, P., Mitchell, A., Apweiler, R., Attwood, T. K., Bateman, A., Bernard, T., Binns, D., Bork, P., Burge, S., de Castro, E., Coggill, P., Corbett, M., Das, U., Daugherty, L., Duquenne, L., Finn, R. D., Fraser, M., Gough, J., Haft, D., Hulo, N., Kahn, D., Kelly, E., Letunic, I., Lonsdale, D., Lopez, R., Madera, M., Maslen, J., McAnulla, C., McDowall, J., McMenamin, C., Mi, H., Mutowo-Muellenet, P., Mulder, N., Natale, D., Orengo, C., Pesseat, S., Punta, M., Quinn, A. F., Rivoire, C., Sangrador-Vegas, A., Selengut, J. D., Sigrist, C. J., Scheremetjew, M., Tate, J., Thimmajanarthanan, M., Thomas, P. D., Wu, C. H., Yeats, C., and Yong, S. Y. (2012) InterPro in 2011: new developments in the family and domain prediction database. *Nucleic Acids Res.* **40**, D306–D312
58. Harris, T. W., Antoshechkin, I., Bieri, T., Blasiar, D., Chan, J., Chen, W. J., De La Cruz, N., Davis, P., Duesbury, M., Fang, R., Fernandes, J., Han, M., Kishore, R., Lee, R., Müller, H. M., Nakamura, C., Ozersky, P., Petcherski, A., Rangarajan, A., Rogers, A., Schindelman, G., Schwarz, E. M., Tuli, M. A., Van Auken, K., Wang, D., Wang, X., Williams, G., Yook, K., Durbin, R., Stein, L. D., Spieth, J., and Sternberg, P. W. (2010) WormBase: a comprehensive resource for nematode research. *Nucleic Acids Res.* **38**, D463–D467
59. Luo, W., and Brouwer, C. (2013) Pathview: an R/Bioconductor package for pathway-based data integration and visualization. *Bioinformatics* **29**, 1830–1831
60. Preston, S., Jiao, Y., Jabbar, A., McGee, S. L., Laleu, B., Willis, P., Wells, T. N., and Gasser, R. B. (2016) Screening of the 'Pathogen Box' identifies an approved pesticide with major anthelmintic activity against the barber's pole worm. *Int. J. Parasitol. Drugs Drug Resist.* **6**, 329–334
61. Cornaglia, M., Krishnamani, G., Mouchiroud, L., Sorrentino, V., Lehnert, T., Auwerx, J., and Gijs, M. A. (2016) Automated longitudinal monitoring of *in vivo* protein aggregation in neurodegenerative disease *C. elegans* models. *Mol. Neurodegener.* **11**, 17
62. Mouchiroud, L., Sorrentino, V., Williams, E. G., Cornaglia, M., Frochaux, M. V., Lin, T., Nicolet-Dit-Félix, A. A., Krishnamani, G., Ouhmad, T., Gijs, M. A., Deplancke, B., and Auwerx, J. (2016) The movement tracker: a flexible system for automated movement analysis in invertebrate model organisms. *Curr. Protoc. Neurosci.* **77**, 1–21, 21
63. Andreux, P. A., Mouchiroud, L., Wang, X., Jovaisaite, V., Mottis, A., Bichet, S., Moullan, N., Houtkooper, R. H., and Auwerx, J. (2014) A method to identify and validate mitochondrial modulators using mammalian cells and the worm *C. elegans*. *Sci. Rep.* **4**, 5285

64. Houtkooper, R. H., Mouchiroud, L., Ryu, D., Moullan, N., Katsyuba, E., Knott, G., Williams, R. W., and Auwerx, J. (2013) Mitonuclear protein imbalance as a conserved longevity mechanism. *Nature* **497**, 451–457
65. Cragg, G. M., and Newman, D. J. (2013) Natural products: a continuing source of novel drug leads. *Biochim. Biophys. Acta* **1830**, 3670–3695
66. Atanasov, A. G., Waltenberger, B., Pferschy-Wenzig, E. M., Linder, T., Wawrosch, C., Uhrin, P., Temml, V., Wang, L., Schwaiger, S., Heiss, E. H., Rollinger, J. M., Schuster, D., Breuss, J. M., Bochkov, V., Mihovilovic, M. D., Kopp, B., Bauer, R., Dirsch, V. M., and Stuppner, H. (2015) Discovery and resupply of pharmacologically active plant-derived natural products: a review. *Biotechnol. Adv.* **33**, 1582–1614
67. Hollingworth, R. M., Ahammadsahib, K. I., Gadelhak, G., and McLaughlin, J. L. (1994) New inhibitors of complex I of the mitochondrial electron transport chain with activity as pesticides. *Biochem. Soc. Trans.* **22**, 230–233
68. Lümmen, P. (1998) Complex I inhibitors as insecticides and acaricides. *Biochim. Biophys. Acta* **1364**, 287–296
69. Sankowsky, N. A. (1936), inventor, Stanco, assignee. Insecticides containing derris extracts and methods of preparing the same. Patent US2058832
70. Murillo, G., Salti, G. I., Kosmeder II, J. W. I. I., Pezzuto, J. M., and Mehta, R. G. (2002) Deguelin inhibits the growth of colon cancer cells through the induction of apoptosis and cell cycle arrest. *Eur. J. Cancer* **38**, 2446–2454
71. Agrawal, R. K., and Sharma, M. R. (2012) Structural aspects of mitochondrial translational apparatus. *Curr. Opin. Struct. Biol.* **22**, 797–803
72. Harder, A. (2016) The biochemistry of *Haemonchus contortus* and other parasitic nematodes. In *Advances in Parasitology* (Gasser, R. B. and and von Samson-Himmelstjerna, G., eds.), Vol. **93**, pp. 69–94, London, UK: Academic Press
73. Kita, K., and Takamiya, S. (2002) Electron-transfer complexes in Ascaris mitochondria. *Adv. Parasitol.* **51**, 95–131
74. Kita, K., Nihei, C., and Tomitsuka, E. (2003) Parasite mitochondria as drug target: diversity and dynamic changes during the life cycle. *Curr. Med. Chem.* **10**, 2535–2548
75. Omura, S., Miyadera, H., Ui, H., Shiomi, K., Yamaguchi, Y., Masuma, R., Nagamitsu, T., Takano, D., Sunazuka, T., Harder, A., Kölbl, H., Namikoshi, M., Miyoshi, H., Sakamoto, K., and Kita, K. (2001) An anthelmintic compound, nafuredin, shows selective inhibition of complex I in helminth mitochondria. *Proc. Natl. Acad. Sci. USA* **98**, 60–62
76. Matsumoto, J., Sakamoto, K., Shinjyo, N., Kido, Y., Yamamoto, N., Yagi, K., Miyoshi, H., Nonaka, N., Katakura, K., Kita, K., and Oku, Y. (2008) Anaerobic NADH-fumarate reductase system is predominant in the respiratory chain of *Echinococcus multilocularis*, providing a novel target for the chemotherapy of alveolar echinococcosis. *Antimicrob. Agents Chemother.* **52**, 164–170
77. Sakai, C., Tomitsuka, E., Esumi, H., Harada, S., and Kita, K. (2012) Mitochondrial fumarate reductase as a target of chemotherapy: from parasites to cancer cells. *Biochim. Biophys. Acta* **1820**, 643–651
78. Andreux, P. A., Houtkooper, R. H., and Auwerx, J. (2013) Pharmacological approaches to restore mitochondrial function. *Nat. Rev. Drug Discov.* **12**, 465–483
79. Dillin, A., Hsu, A. L., Arantes-Oliveira, N., Lehrer-Graiwer, J., Hsin, H., Fraser, A. G., Kamath, R. S., Ahringer, J., and Kenyon, C. (2002) Rates of behavior and aging specified by mitochondrial function during development. *Science* **298**, 2398–2401
80. Tsang, W. Y., and Lemire, B. D. (2002) Mitochondrial genome content is regulated during nematode development. *Biochem. Biophys. Res. Commun.* **291**, 8–16
81. Jovaisaite, V., Mouchiroud, L., and Auwerx, J. (2014) The mitochondrial unfolded protein response, a conserved stress response pathway with implications in health and disease. *J. Exp. Biol.* **217**, 137–143
82. Chen, J. M., Rawlings, N. D., Stevens, R. A. E., and Barrett, A. J. (1998) Identification of the active site of legumain links it to caspases, clostripain and gingipains in a new clan of cysteine endopeptidases. *FEBS Lett.* **441**, 361–365
83. Dalton, J. P., Hola-Jamriska, L., and Brindley, P. J. (1995) Asparaginyl endopeptidase activity in adult *Schistosoma mansoni*. *Parasitology* **111**, 575–580
84. León-Félix, J., Ortega-López, J., Orozco-Solís, R., and Arroyo, R. (2004) Two novel asparaginyl endopeptidase-like cysteine proteinases from the protist *Trichomonas vaginalis*: their evolutionary relationship within the clan CD cysteine proteinases. *Gene* **335**, 25–35
85. Dalton, J. P., and Brindley, P. J. (1996) Schistosome asparaginyl endopeptidase SM32 in hemoglobin digestion. *Parasitol. Today* **12**, 125
86. Tort, J., Brindley, P. J., Knox, D., Wolfe, K. H., and Dalton, J. P. (1999) Proteinases and associated genes of parasitic helminths. *Adv. Parasitol.* **43**, 161–266
87. Sojka, D., Franta, Z., Horn, M., Hajdusek, O., Caffrey, C. R., Mares, M., and Kopácek, P. (2008) Profiling of proteolytic enzymes in the gut of the tick *Ixodes ricinus* reveals an evolutionarily conserved network of aspartic and cysteine peptidases. *Parasit. Vectors* **1**, 7
88. Oliver, E. M., Skuce, P. J., McNair, C. M., and Knox, D. P. (2006) Identification and characterization of an asparaginyl proteinase (legumain) from the parasitic nematode, *Haemonchus contortus*. *Parasitology* **133**, 237–244
89. Skuce, P. J., Redmond, D. L., Liddell, S., Stewart, E. M., Newlands, G. F., Smith, W. D., and Knox, D. P. (1999) Molecular cloning and characterization of gut-derived cysteine proteinases associated with a host protective extract from *Haemonchus contortus*. *Parasitology* **119**, 405–412
90. Redmond, D. L., and Knox, D. P. (2006) Further protection studies using recombinant forms of *Haemonchus contortus* cysteine proteinases. *Parasite Immunol.* **28**, 213–219
91. Knox, D. P. (2007) Proteinase inhibitors and helminth parasite infection. *Parasite Immunol.* **29**, 57–71
92. Lustigman, S., Zhang, J., Liu, J., Oksov, Y., and Hashmi, S. (2004) RNA interference targeting cathepsin L and Z-like cysteine proteases of *Onchocerca volvulus* confirmed their essential function during L3 molting. *Mol. Biochem. Parasitol.* **138**, 165–170
93. Rascón, A. A., Jr., and McKerrow, J. H. (2013) Synthetic and natural protease inhibitors provide insights into parasite development, virulence and pathogenesis. *Curr. Med. Chem.* **20**, 3078–3102
94. Ondrovics, M., Gasser, R. B., and Joachim, A. (2016) Recent advances in elucidating nematode moulting- prospects of using *Oesophagostomum dentatum* as a model. *Adv. Parasitol.* **91**, 233–264
95. Rhoads, M. L., Fetterer, R. H., and Urban, J. F., Jr. (1998) Effect of protease class-specific inhibitors on *in vitro* development of the third- to fourth-stage larvae of *Ascaris suum*. *J. Parasitol.* **84**, 686–690
96. Rhoads, M. L., Fetterer, R. H., and Urban, J. F., Jr. (2001) Cuticular collagen synthesis by *Ascaris suum* during development from the third to fourth larval stage: identification of a potential chemotherapeutic agent with a novel mechanism of action. *J. Parasitol.* **87**, 1144–1149
97. Guiliano, D. B., Hong, X., McKerrow, J. H., Blaxter, M. L., Oksov, Y., Liu, J., Ghedin, E., and Lustigman, S. (2004) A gene family of cathepsin L-like proteases of filarial nematodes are associated with larval molting and cuticle and eggshell remodeling. *Mol. Biochem. Parasitol.* **136**, 227–242
98. Cox, G. N., Kusch, M., and Edgar, R. S. (1981) Cuticle of *Caenorhabditis elegans*: its isolation and partial characterization. *J. Cell Biol.* **90**, 7–17
99. Page, A. P., and Johnstone, I. L. (2007) The cuticle. In *WormBook*, The *C. elegans* Research Community, electronic resource doi:10.1895/wormbook.1.138.1
100. Simmer, F., Moorman, C., van der Linden, A. M., Kuijk, E., van den Berghe, P. V., Kamath, R. S., Fraser, A. G., Ahringer, J., and Plasterk, R. H. (2003) Genome-wide RNAi of *C. elegans* using the hypersensitive *rrf-3* strain reveals novel gene functions. *PLoS Biol.* **1**, E12
101. Frand, A. R., Russel, S., and Ruvkun, G. (2005) Functional genomic analysis of *C. elegans* molting. *PLoS Biol.* **3**, e312
102. Fritz, J. A., and Behm, C. A. (2009) CUTI-1: a novel tetraspan protein involved in *C. elegans* CUTicle formation and epithelial integrity. *PLoS One* **4**, e5117
103. Cerniglia, G. J., Dey, S., Gallagher-Colombo, S. M., Daurio, N. A., Tuttle, S., Busch, T. M., Lin, A., Sun, R., Esipova, T. V., Vinogradov, S. A., Denko, N., Koumenis, C., and Maity, A. (2015) The PI3K/Akt pathway regulates oxygen metabolism *via* pyruvate dehydrogenase (PDH)-E1α phosphorylation. *Mol. Cancer Ther.* **14**, 1928–1938
104. Skinner-Adams, T. S., Sumanadasa, S. D., Fisher, G. M., Davis, R. A., Doolan, D. L., and Andrews, K. T. (2016) Defining the targets of antiparasitic compounds. *Drug Discov. Today* **21**, 725–739

Received for publication April 5, 2017.
Accepted for publication June 12, 2017.

Deguelin exerts potent nematocidal activity *via* the mitochondrial respiratory chain

Sarah Preston, Pasi K. Korhonen, Laurent Mouchiroud, et al.

FASEB J published online July 7, 2017
Access the most recent version at doi:10.1096/fj.201700288R